

# The cephalic anatomy of workers of the ant species *Wasmannia affinis* (Formicidae, Hymenoptera, Insecta) and its evolutionary implications

Adrian Richter<sup>a, \*</sup>, Roberto A. Keller<sup>b, c</sup>, Félix Baumgarten Rosumek<sup>d, e</sup>,  
Evan P. Economo<sup>b</sup>, Francisco Hita Garcia<sup>b</sup>, Rolf G. Beutel<sup>a</sup>

<sup>a</sup> Institut für Zoologie und Evolutionsforschung, Friedrich-Schiller-Universität Jena, 07743 Jena, Germany

<sup>b</sup> Biodiversity and Biocomplexity Unit, Okinawa Institute of Science and Technology Graduate University, Onna-son, Okinawa, 904-0495, Japan

<sup>c</sup> MUHNAC/cE3c –Centre for Ecology, Evolution and Environmental Changes, Faculdade de Ciências da Universidade de Lisboa, 1749-016 Lisbon, Portugal

<sup>d</sup> Ecological Networks, Technische Universität Darmstadt, Darmstadt, Germany

<sup>e</sup> Department of Ecology and Zoology, Federal University of Santa Catarina, Florianópolis, Brazil

## ARTICLE INFO

### Article history:

Received 19 December 2018

Accepted 4 February 2019

### Keywords:

Ants

Head

Morphology

Skeletomusculature

3D-reconstruction

## ABSTRACT

Despite the ecological significance of ants and the intensive research attention they have received, thorough treatments of the anatomy and functional morphology are still scarce. In this study we document the head morphology of workers of the myrmicine *Wasmannia affinis* with optical microscopy,  $\mu$ -computed tomography, scanning electron microscopy, and 3D reconstruction, providing the first complete anatomical treatment of an ant head with a broad array of modern techniques. We discuss the potential of the applied methods to generate detailed and well-documented morphological data sets with increased efficiency. We also address homology problems, particularly in the context of the cephalic digestive tract. According to our analyses the “pharynx” of previous ant studies is homologous to the prepharynx of other insects. We also discuss the phylogenetic potential and functional significance of the observed characters, with internal features such as tentorium and musculature discussed for the first time. Our investigation underlines that detailed anatomical data for Formicidae are still very fragmentary, which in turn limits our understanding of the major design elements underlying the ant *bauplan*. We attempt to provide a template for further anatomical studies, which will help to understand the evolution of this fascinating group on the phenotypic level.

© 2019 Elsevier Ltd. All rights reserved.

## 1. Introduction

The ecological dominance, high biomass, diversity of interactions with other species, and complex eusocial colony structures have brought much well-deserved attention to the ants (Hölldobler and Wilson, 1990). With 13,428 valid species (Bolton, 2018) Formicidae represent “only” about 1% of the total insect species number (Stork et al., 2018). However, ants have evolved a remarkable range of lifestyles and feeding habits. They can be specialized predators, granivores or fungivores, and occur in nearly all types of ecosystems, with the exception of the polar regions, high mountain tops, and aquatic habitats (Hölldobler and Wilson, 1990; Lach et al., 2010). As a result, ants are one of the most intensively investigated insect taxa, with studies on symbioses (e.g.

Russell et al. 2009; Weber, 1972), behaviour (e.g. Hölldobler et al., 1978), chemical ecology (e.g. Cavill et al., 1984), systematics and taxonomy (e.g. Bolton, 2003; Ward et al., 1996), genetics (e.g. Lee et al., 2018) and evolutionary developmental biology (e.g. Abouheif and Wray, 2002), among others. The long-debated evolutionary history of ants has recently been elucidated through phylogenetic analyses for the family as a whole (Moreau et al., 2006; Brady et al., 2006; Ward, 2014; Borowiec et al., 2017) and for the most species-rich subfamilies Dolichoderinae (Ward et al., 2010), Formicinae (Blaimer et al., 2015) and Myrmicinae (Ward et al., 2015).

Considering the intensive research interest on ants, it is surprising that a complete treatment of the cephalic anatomy based on modern techniques is presently not available. This does not mean that the morphology of the group has not been studied intensively. Morphological information on ants addressing features of the external skeleton is presented in studies with a taxonomic (e.g. Bolton, 2003; Boudinot, 2015; Hita Garcia et al., 2017a,b) or a

\* Corresponding author.

E-mail address: [adrichter@gmx.de](mailto:adrichter@gmx.de) (A. Richter).

phylogenetic context (e.g. Brown, 1954; Baroni Urbani et al., 1992; Schultz and Meier, 1995; Brady and Ward, 2005; Brandão and Mayhé-Nunes, 2007; Keller, 2011; Barden et al., 2017), as well as in studies documenting the relatively rich fossil record in amber (e.g. Barden and Grimaldi, 2016; Barden, 2017). Comparative studies on head morphology are available, especially on the mouthparts (Gotwald, 1969, 1970, 1973), the antennal sockets (Keller, 2011), and the antennal sensilla (Hashimoto, 1990). Studies primarily concerned with different aspects of ant biology also contain morphological data on particular ant species (e.g. Currie et al., 2006). However, information on internal structures is scarce to absent in all these studies.

Anatomical data on the head were presented in some publications focussing on the digestive tract, glands, and the musculature of ants (e.g. Forbes, 1938, Whelden, 1957a,b, 1963; Peregrine et al., 1973; Hansen et al., 1999), although the latter is never described in any detail. Of these, only Peregrine et al. (1973) tried to identify different muscles of the cephalic digestive tract and to specify their origin and insertion. The most comprehensive anatomical studies covering the skeleto-muscular system in some detail are due to the remarkable efforts of some early pioneers, including Claude Janet (e.g. Janet, 1899, 1905) and John Lubbock (1877). The illustrations from these works are impressive given the instruments available at the time, but details on the insertions, areas of origin, and three-dimensionality of structures are missing for many muscles. The mandibular musculature of ants has been studied more intensively than all other cephalic muscles (e.g. Gronenberg et al., 1997; Paul and Gronenberg, 1999; Paul, 2001; Muscedere et al., 2011; Khalife et al., 2018), particularly for trap-jaw ants (e.g. Brown and Wilson, 1959; Gronenberg, 1995; Gronenberg, 1996; Gronenberg and Ehmer, 1996; Gronenberg et al., 1998a; Larabee et al., 2017), and recently snap-jaw ants (Larabee et al., 2018). Other muscles of the head have also been covered in an investigation with a functional focus (Paul et al., 2002). Altogether, the presently available information on the cephalic anatomy of ants can be described as fragmentary, leaving many questions open about the exact origin, insertion and shape of the multitude of muscles that operate inside the head. Few anatomical studies on other body parts of ants are available. For example, Saini et al. (1982) and Liu et al. (2019) investigated the mesosoma, Hashimoto (1996) and Perrault (2005) the anterior metasoma, and Boudinot (2013) the male genitalia.

The primary aim of the present study is to document in detail the complete cephalic anatomy of workers using a broad array of techniques. We focus on *Wasmannia affinis* Santschi, 1929, a species that occurs in the Atlantic forests of southeastern Brazil (Longino and Fernández, 2007; Janicki et al., 2016) and has generalist feeding habits, including small arthropods, sugars, seeds and fallen fruits (Rosumek, 2017). The genus *Wasmannia* is mainly known by the invasive species *Wasmannia auropunctata* (Roger, 1863), which causes ecological and economic damage in many tropical and subtropical regions (e.g. Clark et al., 1982; Jourdan, 1997; Wetterer and Porter, 2003). In terms of its morphology, *Wasmannia* is a non-specialized representative of the subfamily Myrmicinae, which contains half of the known ant species and the richest diversity within the family. This can be considered as a template for future studies involving a broader array of ant species and castes. Well-documented data on the external and internal morphology will not only be useful for phylogenetic analyses or plausibility checks of molecular phylogenies, but also help to reconstruct the character evolution in Formicidae on the phenotypic level. This will allow comparisons with other groups of insects, for which such data are already available (e.g. Zimmermann and Vilhelmsen, 2016; Beutel et al., 2017), and improve our understanding of the major innovations in functional morphology of ants. Extensive data from

the literature are taken into consideration, not only covering ants but also other groups of Hymenoptera, especially representatives of the Aculeata.

The detailed investigation of the skeleto-muscular apparatus of the head of this species is a first step towards an optimized and standardized anatomical documentation of heads of ants in general. We discuss the possible application of a broad array of techniques to reach this goal, most of which were employed in this work. Some homology issues are addressed, especially concerning the digestive tract. Finally, we discuss cephalic character transformations, including their functional implications, which may have played a role in the early evolution of this extraordinarily successful group of insects (Hölldobler and Wilson, 1990; Grimaldi and Engel, 2005).

## 2. Material and methods

### 2.1. Material

Workers of *W. affinis* were collected at the Desterro Conservation Unit, Florianopolis, Brazil, in January 2016 and preserved in 70% ethanol. For details concerning collection methods and species identification see Rosumek (2017). Twelve workers (11 + 1 for  $\mu$ CT) of *W. affinis* were used for the present study. Additionally, several workers of *Acromyrmex aspersus* (Smith, F., 1858), collected in the same manner, were treated with the same methods described here. The results of these investigations will be published at a later date, but they are used as comparison at several points in the discussion of this work.

### 2.2. Sample preparation

The heads of three specimens of *W. affinis* were separated from the body with Dumont No. 5 forceps. Two heads of *W. affinis* were treated with ultra-sonic sound (Sonorex device Type RK 31, Bاندelin electronics, Berlin, Germany) for 2 min. The heads were transferred via an ascending ethanol series (70, 80, 90, 96, 100%) into 100% acetone. Next, Critical Point Drying in liquid CO<sub>2</sub> was performed with an Emitech K 850 Critical Point Dryer (Sample Preparation Division, Quorum Technologies Ltd., Ashford, England).

One of the heads was treated overnight with Scheerpeltz solution (65% ethanol, 5% acetic acid and 30% aqua dest) to soften the antennae, which were then fixed in a more suitable position with minutiae needles. The sample was then transferred to 100% EtOH overnight, and subsequently in 100% acetone. Finally, it was dried at the critical point as described above, and then mounted on minutiae with super glue. The three heads were fixed in different positions and used for Photomicrography and SEM.

One specimen was treated in a slightly heated (ca. 25–30 °C) KOH solution for several hours. After rinsing the sample in distilled water, its mouthparts were dissected under a stereomicroscope (Leica MZ 125) using Dumont forceps and sharpened minutiae glued to glass pipettes or mounted on a craft knife holder (Max Bringmann KG, Wendelstein, Germany). Additionally, one head was dissected without prior treatment with KOH. The isolated mouthparts were placed in microporous sample chambers and transferred to 100% non-denaturated ethanol (70, 80, 96, 100%), and dried at the critical point. The minute mouthparts were attached to SEM stubs with double sided adhesive film. One partly dissected head was macerated overnight at 50 °C in KOH solution. After finishing the preparation of the mouthparts it was cleaned with ultra-sonic sound three times (5 s) to obtain a clear view of the oral foramen. The head and dissected mouthparts were then dried at the critical point as described above and glued on minutiae.

### 2.3. Scanning electron microscopy

Samples were mounted on a rotatable specimen holder (Pohl, 2010). An Emitech K 500 (Sample Preparation Division, Quorum Technologies Ltd., Ashford, England) was used for sputter coating with gold. SEM micrographs were taken with a Philips ESEM XL30 (Philips, Amsterdam, Netherlands) equipped with Scandium FIVE software (Olympus, Münster, Germany). In order to increase the depth of field, some image series with different focus were combined with Helicon Focus 6 (Helicon Soft Inc., Roseau Valley 00152 Dominica).

### 2.4. Microtome section series

Gaster, legs and antennae of a specimen were removed with Dumont forceps. Two additional specimens were severed in the prothoracic region with the same forceps and their antennae removed to achieve better penetration of the embedding medium. Dehydration of the samples was performed as described for drying at the critical point, followed by embedding in Araldite CY 212 (Agar Scientific, Stansted/Essex, England). The samples were sectioned (1  $\mu\text{m}$  thickness) with a microtome HM 360 (Microm, Walldorf, Germany) equipped with a diamond knife. The first head was sectioned horizontally. Cross sections and longitudinal sections were made using the other two heads. The longitudinal section was partly done with a glass knife (1.5  $\mu\text{m}$ ). The sections were stained with toluidine blue and pyronine G (Waldeck GmbH & Co. KG/Chroma Division, Münster, Germany) and examined with an Axioscope (Carl Zeiss AG, Oberkochen, Germany). To document selected sections, pictures were taken with an Olympus dot. Slide microscope (BX51, software version 3.4, Olympus, Tokyo, Japan).

### 2.5. Micro-computed tomography scanning

A micro-CT scan of one specimen dried at the critical point was performed at the beamline P05 in Petra III, DESY (Hamburg), with a magnification of 18.003613 and 12 keV, yielding a voxel size of 0.66  $\mu\text{m}$ . The scans were reconstructed as a Tiff image series. The  $\mu\text{CT}$ -Scan data were uploaded to the dryad online repository and are freely available (Richter et al. 2019; <https://doi.org/10.5061/dryad.911161j>).

### 2.6. 3D modelling

The  $\mu\text{CT}$  data sets were imported into Amira 6.0 (Visage Imaging GmbH, Berlin, Germany) and segmented with this program. Various structures were marked as materials and exported with the plugin script “multiExport” (working group Frank Friedrich, University of Hamburg) in Amira 6.1 as Tiff image stacks. The image series were then imported in VG-Studio Max 2.0 (Volume Graphics GmbH, Heidelberg, Germany) to create volume renders (Phong) of individual structures.

### 2.7. Photomicrography

Images of dried heads glued to minutia were taken with a Canon EOS 7 D Mark II equipped with a Nikon M Plan 20 0.4 ELWD, in combination with a bellows device. The samples were illuminated by two flashes through a transparent plastic cylinder for soft light. Zerene Stacker (Zerene Systems LLC, Richland, USA) was used to combine image stacks with a different focus. All prepared mouthparts were placed on a slide in 70% EtOH or distilled water prior to drying and covered with a coverslip with kneading beads at the corners. The prepared samples were photographed with transmitted light on a Keyence VHX 2000 (Keyence Deutschland GmbH,

Neu-Isenburg) digital microscope. Images of the dried mouthparts were produced under reflected light with the same microscope. They were not mounted as image plates due to insufficient quality, but provided information on colouration, also allowing tentative interpretations of degrees of sclerotization of different areas of the mouthparts.

### 2.8. Image processing

All images were edited with Adobe Photoshop® CS6 (Adobe System Incorporated, San Jose, USA) and arranged into figure plates. On SEM images and images from section series tonal correction was performed. In addition, the selective sharpener was used, also in the case of photomicrographs. Adobe Illustrator® CS6 (Adobe Systems Incorporated, San Jose, USA) was used to label the figure plates.

### 2.9. Terminology

The myrmecological terminology is based on Keller (2011), the general anatomical terminology on Beutel and Vilhelmsen (2007) and Beutel et al. (2014). The definition of “suture” and “internal strengthening ridge” is originally based on Wipfler et al. (2011). The lateral process of the mandible is called abductor swelling following Michener and Fraser (1978). Terms for structures of the maxillolabial complex not previously described in ants are taken from Popovici et al. (2014). Positional designations were partially modified to account for ant prognathism (e.g., “dorsal” and “ventral” sclerites of the glossa were used for ants whereas “anterior” and “posterior” sclerite are used in hypognathous hymenopterans). The glands were named after Grasso et al. (2004), two glands were renamed according to the newly established homology of parts of the digestive tract (see results section). An overview of important terms used in this work is provided in Table 2, Appendix B.

## 3. Results

### 3.1. Head capsule

The head of *W. affinis* workers is prognathous; it appears subtriangular in dorsal view (Figs. 1A and 2A) and is longer than wide; the hind margin of the head is slightly concave and the sides convex; it reaches its maximum width shortly posterad the compound eyes; in lateral view it appears subrectangular, with an evenly convex dorsal surface (Figs. 1B and 2B); the ventral side is only distinctly convex anteriorly, whereas the posterior 1/3 is flat. The cervical articulation with the prothorax is very narrow; the foramen occipitale is also strongly narrowed and deeply counter-sunk in the occipital region; the strongly sclerotized postocciput encloses it in a collar-like manner (Figs. 1C and 2C, F); it is connected with the pronotum and the propleura by a cervical membrane; an articulatory concavity is present ventrolaterally. The posterior tentorial pits are recognizable laterad the foramen (ptp, Figs. 1C and 2C, F). The ventral closure of the head is formed by a postgenal bridge. The internal postgenal ridge is visible as a darker line on photomicrographs (pgr, Fig. 1C) (this character is commonly referred to as postgenal suture, but it is in fact an internal strengthening ridge). Some of the setae inserted on the head capsule show a conspicuous dentation (Fig. 2H). Distinct frontal carinae extend from the antennal insertions to the area of the vertex (frc, Figs. 1A and 2A). The cuticle is uniformly bronze-coloured, with only the carinae and ridges appearing darker. The compound eyes are drop-shaped, with the narrower side anteriorly oriented; they are composed of 36 ommatidia, some of them with short setae inserted between them (Fig. 2G). The antennal scrobe, a

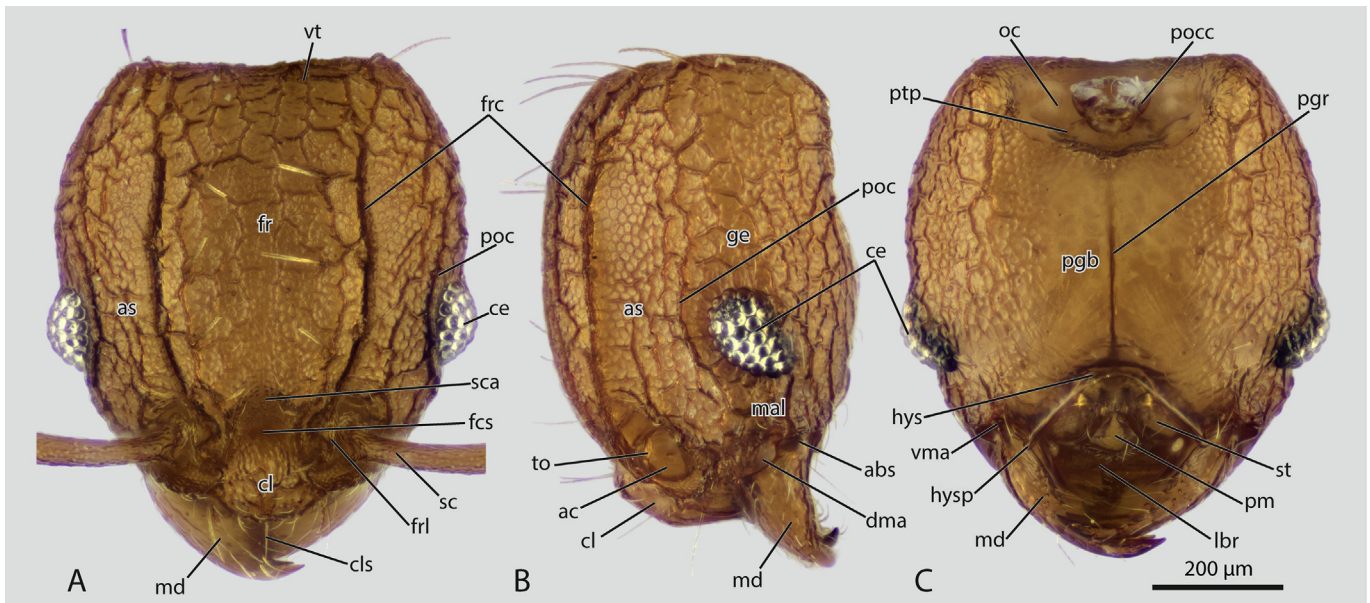


**Fig. 1.** Photomicrographs of the head of *W. affinis*. **A.** Dorsal view. **B.** Lateral view. **C.** Ventral view. Abbreviations: **abs** — abductor swelling, **ac** — acetabulum, **as** — antennal scrobe, **ce** — compound eye, **cl** — clypeus, **dma** — dorsal mandibular articulation, **fcs** — frontoclypeal sulcus, **fr** — frontal area, **frc** — frontal carina, **frl** — frontal lobe, **ge** — gena, **hys** — hypostoma, **hysp** — hypostomal process, **lbr** — labrum, **mal** — malar region, **md** — mandible, **oc** — occipital region, **pgb** — postgenal bridge, **pgr** — postgenal ridge (visible through the head capsule), **pm** — prementum, **poc** — preocular carina, **pocc** — postocciput, **ptp** — posterior tentorial pit, **sc** — scape, **sca** — supraclypeal area, **st** — stipes, **to** — torulus, **vma** — ventral mandibular articulation, **vt** — area of the vertex.

very flat furrow above the eyes between the antennal insertion and the area of the vertex, is delineated by the frontal carina dorsally and the preocular carina ventrally (as, Figs. 1A, B and 2A, B). The clypeus is distinctly extended posteriorly between the antennal insertions; the frontoclypeal strengthening ridge is present as a distinct furrow (fcs, Fig. 2E), with a rounded-triangular supra-clypeal region just posterior to it (sca, Fig. 2E); the clypeus is distinctly convex just compared to the frontal area; its anterior portion is distinctly bent downwards and nearly vertical, whereas its posterior part runs parallel to the anterior frontal region in lateral view; posterolaterally the clypeus is delimited by the anterior tentorial pits, located laterad the antennal insertion area within concavities of the cuticle in this region (atp, Fig. 3E). The clypeus bears a distinct unpaired anteromesal seta (cls, Figs. 1A and 2A). The hypostoma is distinct and broad. It is slightly elevated compared to the postgenal surface and anteriorly directed (hys, Figs. 1C, 2C and 10C), apically rounded processes extend over the ventral bases of the mandibles laterally (hysp, Figs. 1C and 2C). The hypostoma forms a distinct concavity together with the distal postgenae, which receives the proximal parts of the maxillolabial complex (Figs. 9I, L and 10C, F). The antennal insertions are deeply countersunk into peritorular grooves (ptg, Fig. 3D); the median arch of the ring-shaped torulus is extended as a posterolateral lobe which distinctly overlaps and covers the antennal insertion (trm, Fig. 3D, E); the anterior section of the frontal carina is slightly extended as a frontal lobe laterally and partly covers the torulus dorsally (frl, Figs. 1A, 2A and 3D, E); the bulbus of the scapus is inserted in a globular acetabulum formed by the torulus but is not completely enclosed by it (ac, Figs. 1B, 2B and 3D, E).

### 3.2. Endoskeleton

The very long anterior tentorial arms (ata, Figs. 10A–C, 11 and 12) extend from the occipital region almost to the level of the antennal insertions. They are thin but bear mesally directed lamellae in the central region of the head (ml, Fig. 10A–C); these

extensions are widening anteriorly and extend from about the middle region of the head to the level of the anterior edge of the compound eyes. The posterior arms (pta, Figs. 10A, B and 11G) are very short. The tentorial bridge (tb, Figs. 10A–C and 11G) originates directly from the tentorial base at the posterior head capsule; it is a thin crossbeam with an anteriorly directed angle and a median process at the anterior edge, which is continuous with the tendon of M. 48/50. Dorsal tentorial arms are missing and a secondary tentorial bridge (e.g. Zimmermann and Vilhelmsen, 2016) is also absent, and also processes of the posterior tentorium. A postgenal ridge is present on the ventral side of the head capsule (pgr, Fig. 10C). It originates from the hypostoma and slightly reaches beyond the central region of the head. Its upper edge forms a plateau in the anterior third and posteriorly its height decreases continuously. The acetabulum of the antennal insertion is extended as a wide phragma internally (aphr, Fig. 10C), which serves as attachment area for a component of the frontohypopharyngeal muscle (M41a).

### 3.3. Antennae

The antennae insert in laterally oriented concave articulatory areas on the dorsal side of the head capsule directly behind the clypeus. The bulbus (bb, Fig. 3A, C) of the scapus (sc, Fig. 3A) is deeply countersunk in the acetabulum (ac, Fig. 3D, E) and therefore only partly visible; it articulates with a peg-like antennifer, which originates in the deep middle region of the acetabulum, shortly before this connects with the lumen of the head capsule. The very long scapus is almost half as long as the entire antenna; the strongly flattened semiglobular bulbus bears a short shaft-like bulbus neck; this structure is separated from the remaining scapus by a collar which is distinctly extended posteriorly (scp, Fig. 3A); the collar dorsally covers a large part of the antennal insertion area. The pedicellus (pd, Fig. 3A), the proximal element of the funiculus, attaches to the apical articulatory area of the scapus; it articulates with the frontal side of the scapus and is proximally



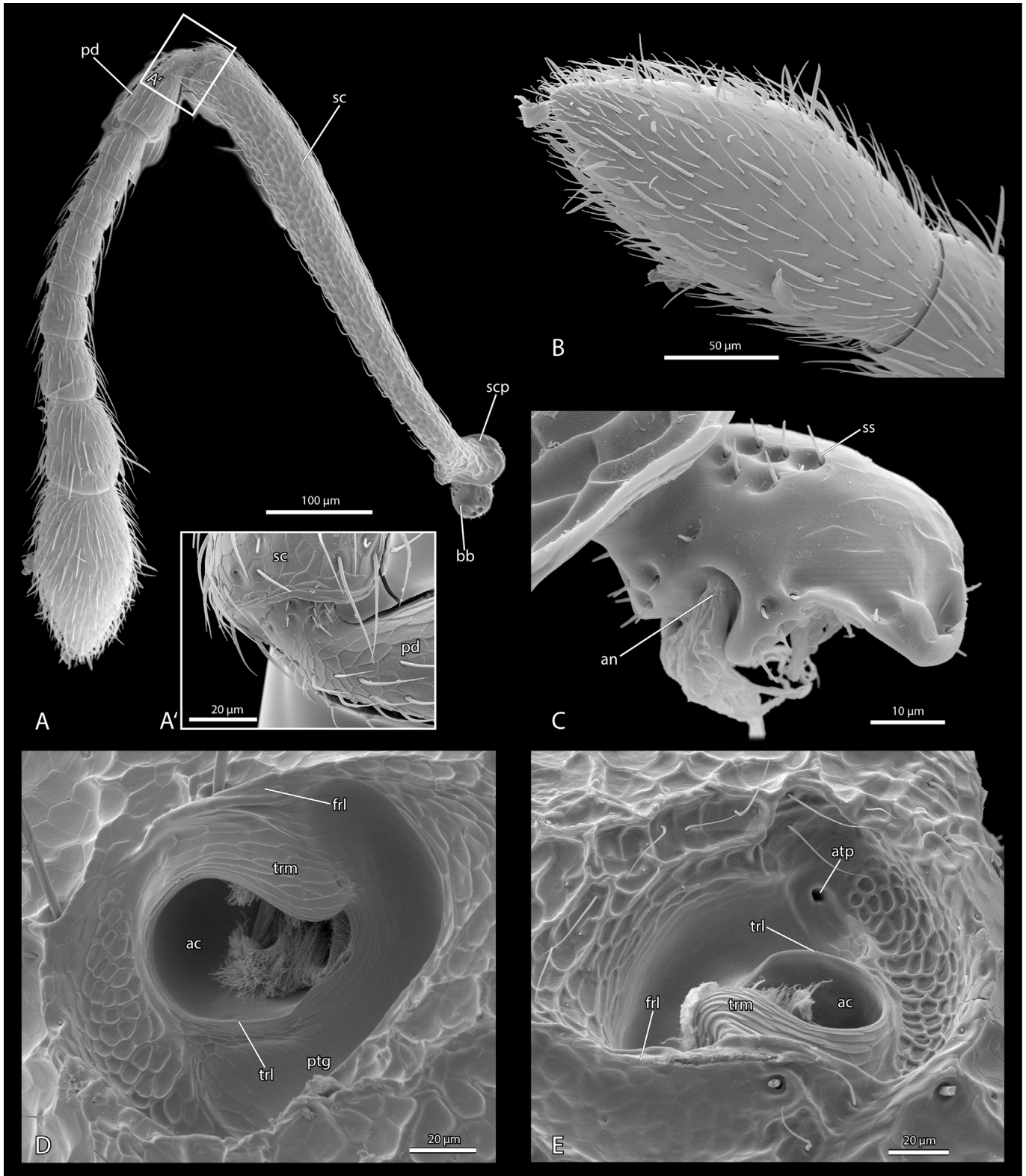


**Fig. 3.** SEM images of the antenna (A–C) and antennal insertion areas (D, E) of *W. affinis*. **A.** Antenna in dorsal view. **A'.** Contact zone of scape and pedicel. **B.** Apical antennomere in ventral view. **C.** Bulbus of the antenna in frontoventral view. **D.** Antennal insertion area in lateral view. **E.** Antennal insertion area in dorsal view. Abbreviations: **ac** – acetabulum, **an** – anterolateral notch of the bulbus, **atp** – anterior tentorial pit, **bb** – bulbus of the scape, **frl** – frontal lobe, **pd** – pedicel, **ptg** – peritorular groove, **sc** – scape, **scp** – collar of the scapal base, **ss** – short setae on the bulbus, **trl** – lateral arch of the torulus, **trm** – mesal arch of the torulus.

bent anterad, which results in the geniculate shape of the antenna; it is strongly narrowed in its articular area but widens distally. The first true flagellomere is slightly longer than the second; the

flagellomeres then increase in length and 6 is longer than the first one; the proximal flagellomeres are narrower than the distal part of the pedicellus; the last three flagellomeres (7–9) are longer than

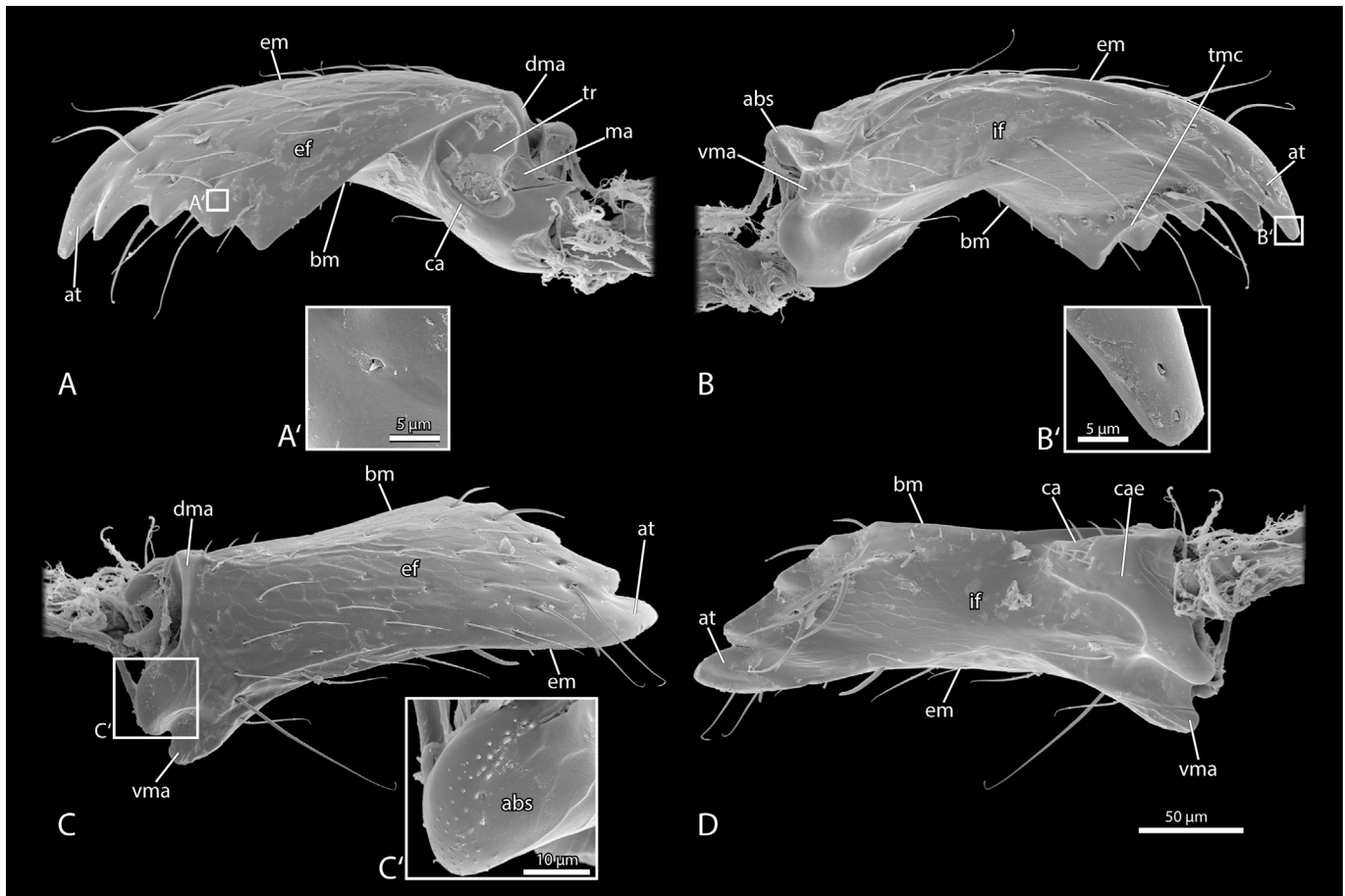


**Fig. 4.** SEM-images of the mandible of *W. affinis*. **A.** Dorsal view. **A'.** Sensilla basally on the fourth tooth. **B.** Ventral view. **B'.** Ventral sensilla on the apical tooth. **C.** Lateral view. **C'.** Mandibular process of the abductor apodeme in dorsolateral view. **D.** Mesal view. Abbreviations: **abs** – abductor swelling, **at** – apical tooth, **bm** – basal margin, **ca** – canthellus, **cae** – canthellar elevation, **dma** – dorsal mandibular articulation, **ef** – external mandibular face, **em** – external margin, **if** – internal face of the mandible, **ma** – mandalus, **tmc** – apical transverse mandibular carina, **tr** – trulleum, **vma** – ventral mandibular articulation.

the others and distinctly widening towards the apex, thus forming an indistinct club. The whole antenna, especially the flagellum, carries a lot of setae which are especially densely distributed on the apical antennomere (Fig. 3B).

**Musculature (Figs. 9D–F and 11):** The scapus is moved by four muscles of similar size. The tendons of M. 1 and M. 4, and M. 2 and M. 3, respectively, are running very close to each other over a part of their length (though recognizable as separate structures on microtome sections). **M. tentorioscapalis anterior (M. 1):** Origin (=O): dorsolateral surface of the anterior tentorial arm; Insertion (=I): anterolaterally in a notch of the bulbus, seemingly externally but covered by a membrane (an, Fig. 11C). **M. tentorioscapalis posterior (M. 2):** O: posterodorsal surface of the anterior tentorial arms and extensively on its mesal lamella; I: posterior on the bulbus of the scapus. **M. tentorioscapalis lateralis (M. 3):** O: middle region of the dorsal surface of the anterior tentorial arms, laterad M. 2 and posterad M. 1; I: laterally on the bulbus, seemingly on the external surface but covered by a membrane, posterad M. 1. **M. tentorioscapalis medialis (M. 4):** O: on the mesal lamella of the anterior tentorial arm, mesad M. 1; I: medially on the anterior region of the bulbus. **M. scapopedicellaris lateralis (M. 5)** and **M. scapopedicellaris medialis (M. 6):** (not shown on figure plates) both muscles are present; the precise shape, orientation and insertion sites could not be clarified with the data at hand, but they are likely two narrow bundles, probably with long tendons, originating on the collar-like extension of the proximal scapus.

### 3.4. Mandibles

The basal articulatory area of the mandible is tightly connected with different structures of the head capsule, in addition to the primary and secondary joint; the dorsal (secondary) mandibular joint is formed by a ventrolateral, longitudinal smooth elongation of the clypeus (dma, Fig. 2D), which articulates with a smooth dorsolateral area on the mandibular base (dma, Fig. 4A, C); the ventral (primary) mandibular joint is formed by a narrower, shorter, distally rounded and smooth articular process (vma, Fig. 4B–D), which corresponds with an articular socket of the head capsule (vma, Fig. 2D); an additional well-developed rounded process, the abductor swelling (abs, Fig. 4B, C), is located above and laterad the articular process and internally connected with the abductor apodeme; the mesal edge of the ventral articular socket is a rounded-triangular extension which fits into a shallow mandibular groove; mesad of the ventral socket a large triangular extension of the postgena is in contact with the mandible anterad a low convexity of the mesal mandibular base, closing the ventral part of the foramen (pgt, Fig. 2D); additionally, the dorsal side of the mandible is in contact with a flattened triangular process of the clypeus equipped with a row of setae (vclp, Fig. 2D); when the mandibles are closed it lies behind the basal mandibular margin at the level of the trulleum. The external side of the mandible appears triangular in dorsal view (ef, Fig. 4A); it appears bent mesad to form a large horizontal blade so that the masticatory margin forms an

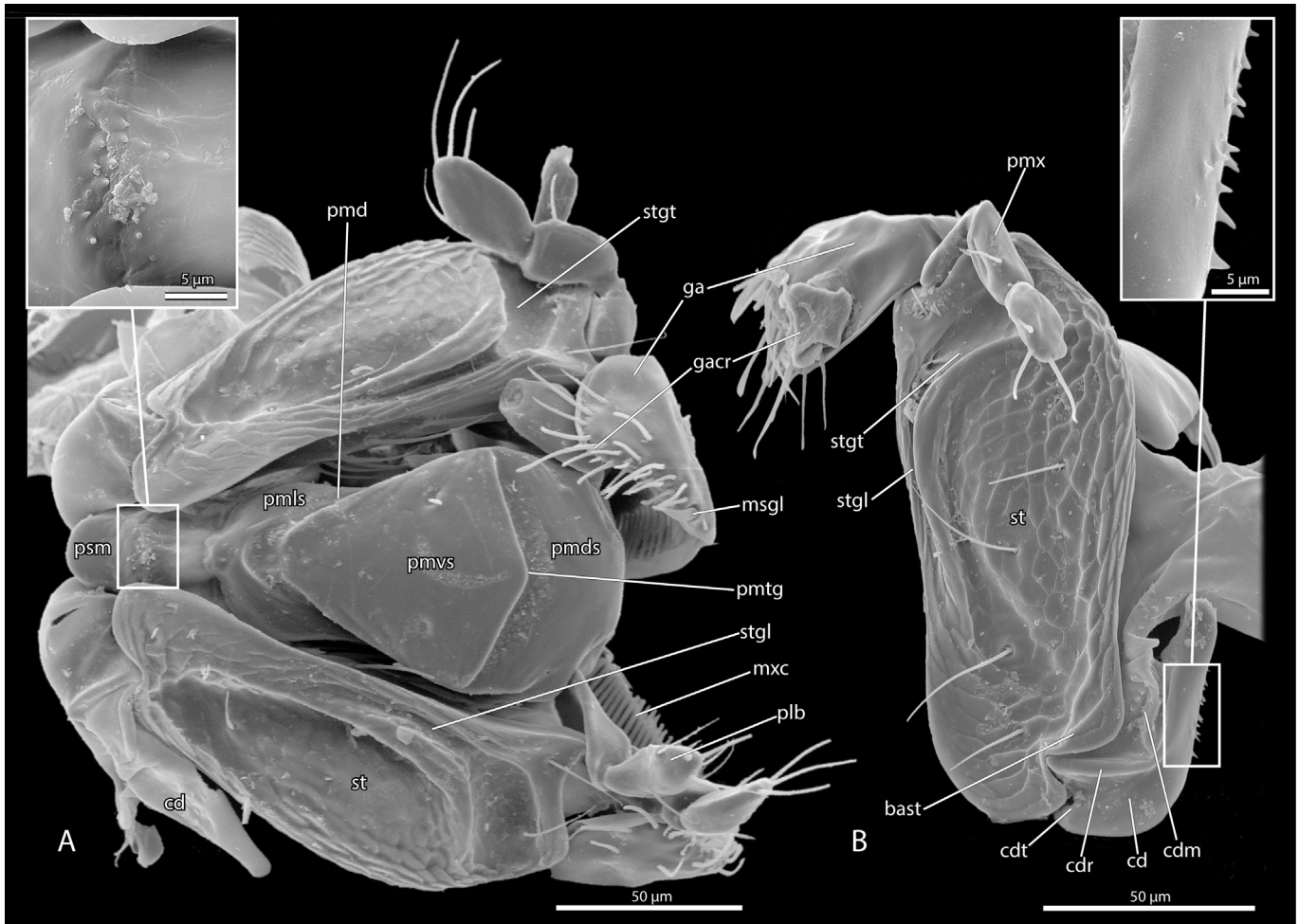


**Fig. 5.** SEM-images of the maxillolabial complex and left maxilla of *W. affinis*. **A.** Maxillolabial complex in ventral view, box: detail of the membrane between postmentum and prementum. **B.** Left maxilla in ventral view, box: denticles on the cardo. Abbreviations: **bast** — basal angle of the stipes, **cd** — cardo, **cdm** — membrane between cardo and stipes, **cdr** — cardinal ridge, **cdt** — cardinal tip, **ga** — galea, **gacr** — galeal crown, **msgl** — median seta of the galeal crown, **mxl** — maxillary comb, **plb** — labial palp, **pmd** — premental ditches, **pmds** — distal surface of the prementum, **pmls** — lateral premental face, **pmtg** — transverse premental groove, **pmvs** — ventral premental face, **pmx** — maxillary palp, **psm** — postmentum, **st** — external stipital sclerite, **stgl** — stipital groove, longitudinal aspect, **stgt** — stipital groove, transverse aspect.

angle of ca. 45° with the axis of mandible rotation; it can be described as torqued (see Keller, 2011, Char. 29), although not by full 90°; the four teeth on the masticatory margin decrease in thickness proximad, and the masticatory margin itself forms a strongly pronounced angle with the basal mandibular margin (bm, Fig. 4); the basal margin extends from the apex of the proximal tooth to the socket of the dorsal (secondary) mandibular articulation in an evenly curved line (bm, Fig. 4A); in contrast, the ventral external margin extends from the ventral joint in an even curve mesad towards the tip of the apical tooth (em, Fig. 4B–D). On the internal face of the mandible, an apical transverse carina runs from the proximal margin of the preapical tooth and almost reaches the angle with the basal margin (tmc, Fig. 4B). An approximately heart-shaped concavity anterad the articulatory area constitutes the trulleum at the basal mandibular region (tr, Fig. 4A); the mandulus is a membranous lobe in a furrow close to this deepening (ma, Fig. 4A); medially the trulleum is delimited by a cuticular ridge, the canthellus (ca, Fig. 4A, D), which is connected to an elevation at the medial base of the mandible (cae, Fig. 4D).

**Musculature (Figs. 9A–C, 11 and 12):** *M. craniomandibularis internus* (**M. 11**): by far the largest muscle of the head. O (= Origin): with many bundles in the posterior 1/2 of head capsule, lateral, ventral and posterior wall of head capsule, anterior bundles

reaching the level of the compound eyes, posterior bundles further ventrad, with the level of the attachment sites declining in an oblique line; I (= insertion): strongly developed apodeme dorso-medially attached on the mandible, shaped like a flat band anteriorly; anteriorly with a small lateral process and posteriorly split into two thinner subcomponents, thus appearing tripartite; additionally, numerous minute cuticular fibrillae connect the fibres of M.11 with the apodeme; posterad the anterior process a bundle from the lateral region and a medioventral bundle insert directly on the band-shaped area of the apodeme; their sarcomeres appear distinctly shorter on the sections than those of the other fibres. *M. craniomandibularis externus* (**M. 12**): distinctly smaller than M. 11. O: ventromedian region of the head capsule and on the entire postgenal ridge. I: thin tendon attached on ventrolateral mandibular process. *M. hypopharyngo-mandibularis* (**M. 13**): extremely thin. O: ventrolaterally from the anterior tentorial arm shortly behind the anterior tentorial pit; I: dorsomesally on the inner surface of the mandible.

### 3.5. Maxillae

The maxillae form a compact functional unit with the labium, the maxillolabial complex (Fig. 5A); the proximal parts of the ventral

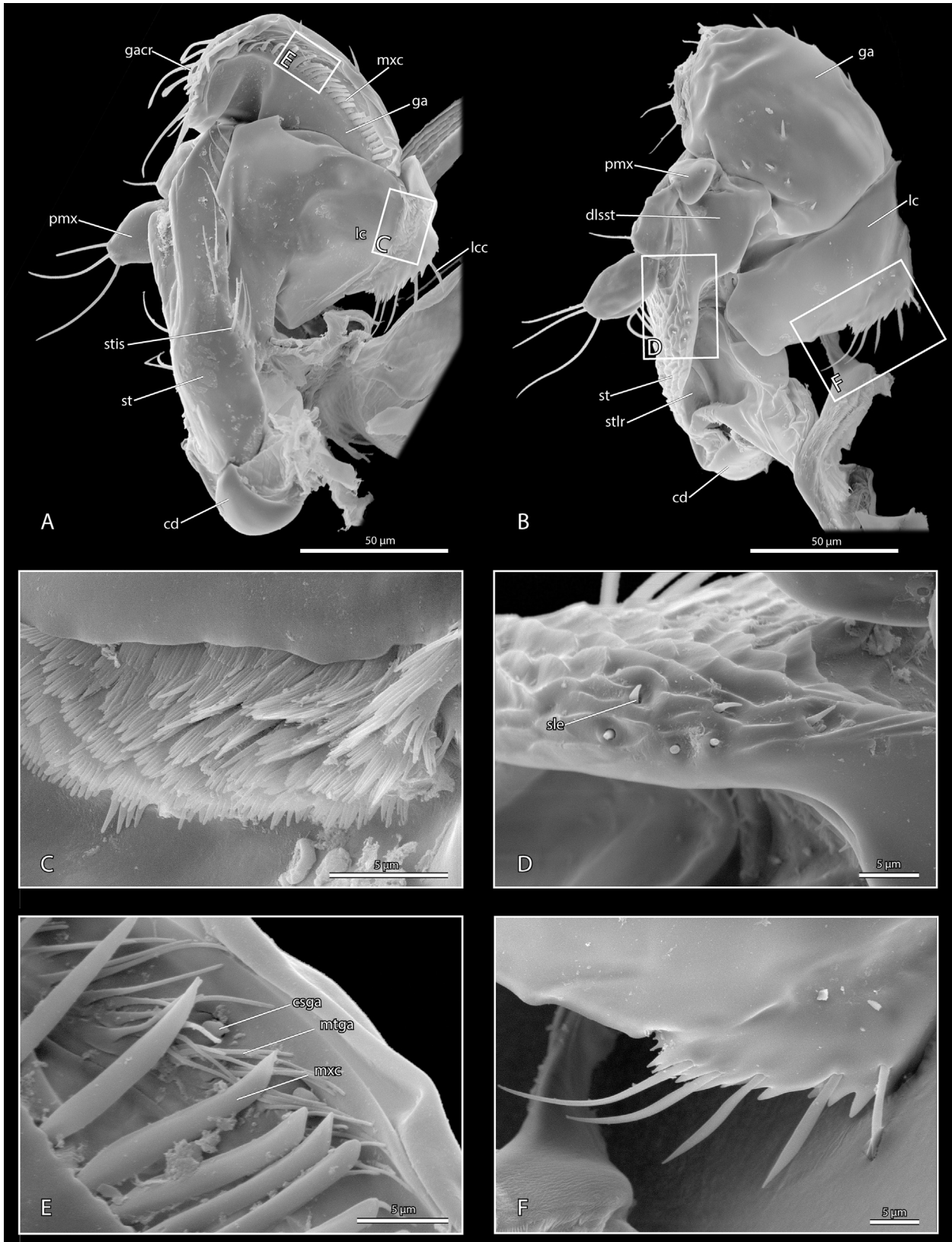


**Fig. 6.** SEM-images of the maxilla of *W. affinis*. **A.** Right maxilla, medioposterior view. **B.** Left maxilla, lateroanterior view. **C.** Microtrichia on the inner side of the lacinia. **D.** Lateral margin of the external stipital sclerite. **E.** Detail of the inner side of the galea. **F.** Lacinial comb. Abbreviations: **cd** — cardo, **csga** — conical sensilla of the galea, **dlsst** — distal lateral margin of the external stipital sclerite, **ga** — galea, **gacr** — galeal crown, **lc** — lacinia, **lcc**, lacinial comb, **mtga** — row of thin setae on the inner side of the galea, **mxc** — maxillary comb, **pmx** — maxillary palp, **sle** — small sensilla at the lateral margin of the external stipital sclerite, **st** — stipes/external stipital sclerite, **stis** — row of setae on the mesal margin of the external stipital sclerite **stlr** — lateral ridge of the external stipital sclerite.

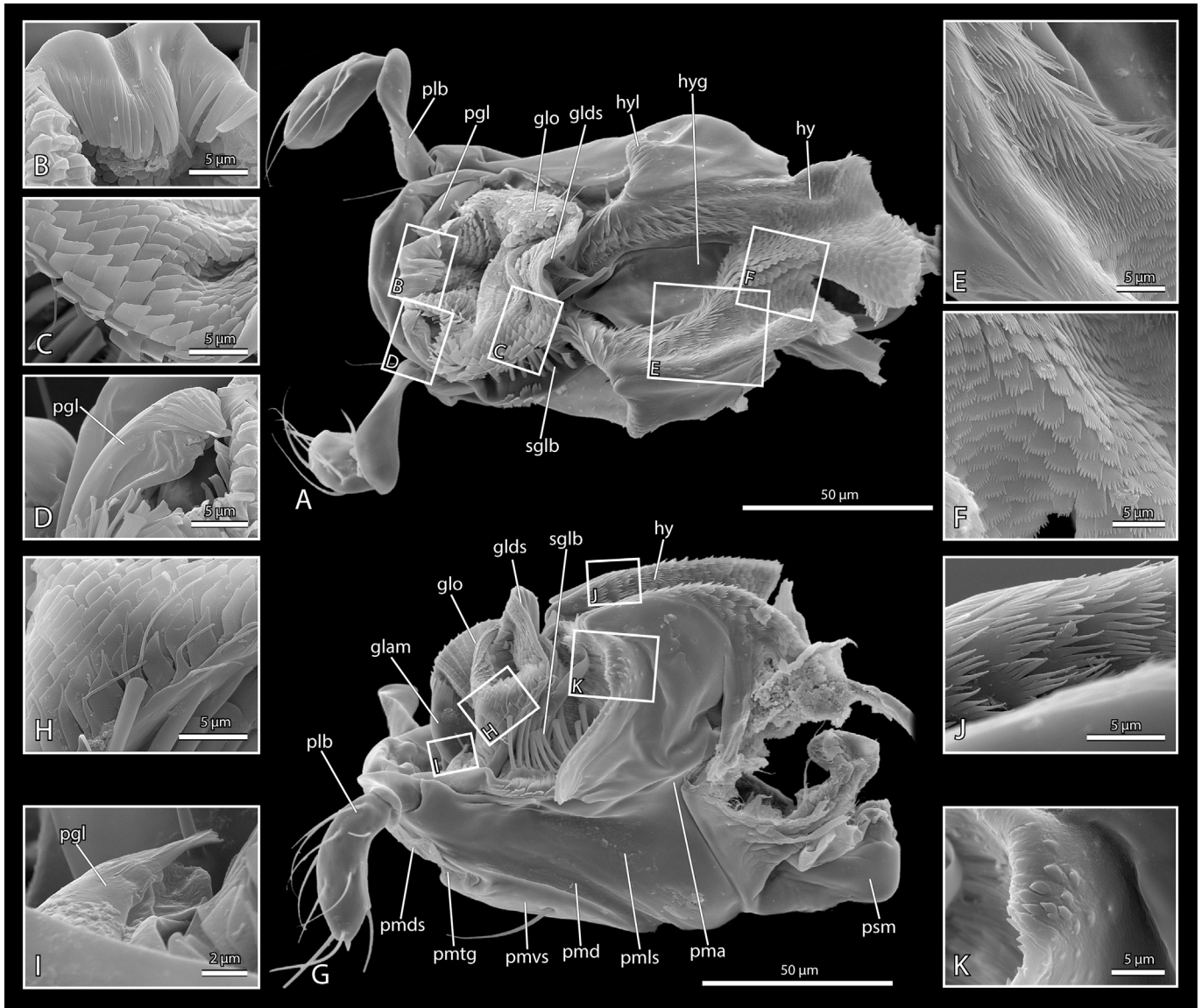


**Fig. 7.** SEM images of the labium of *W. affinis*. **A–F.** Dorsal view, **H–K.** Lateral view. **A.** Overview of the labium and labial part of the hypopharynx. **B.** Anteromedian edge of the glossa. **C.** Detail of the glossa. **D.** Paraglossa. **E.** Distal surface of the hypopharynx. **F.** Proximal surface of the hypopharynx. **G.** Overview of the labium and the labial part of the hypopharynx. **H.** Detail of the glossa. **I.** Paraglossa. **J.** Detail of the distal hypopharynx. **K.** Anterolateral margin of the hypopharynx. Abbreviations: **glo** – glossa, **glam**, anterior median margin of the glossa, **glds** – dorsal sclerite of the glossa, **hy** – hypopharynx, **hyg** – hypopharyngeal groove, **hyl** – lateral anterior margin of the hypopharynx, **pgl** – paraglossa, **plb** – labial palp, **pma** – premental arm, **pmd** – lateral groove of the prementum, **pmds** – distal ventral face of the prementum, **pmls** – lateral premental face, **pmtg**, transverse premental groove, **pmvs** – proximal ventral surface of the prementum, **psm** – postmentum, **sglb** – subglossal brush.

mouthparts are connected with each other by membranes; the entire complex is linked with the head capsule in the hypostomal region, with the cardines inserted in fossae at the anterior margin of the postgenae; the proximal region of the stipes is also connected with the head capsule by a membrane; in the resting position the entire maxillolabial complex is tightly retracted in the foramen orale, with the distal part covered by the labrum (Figs. 1C and 2C); additionally, the entire complex is anteriorly overtopped by the mandibles; laterally and ventrally it is tightly enclosed by the hypostoma. The longitudinal cardo (cd, Figs. 5 and 6A, B) is almost vertically oriented in its retracted position; proximally it is approximately T-shaped, with the lateral arm longer than the mesal one; distally it is bent mesad; its tip (cdt, Fig. 5B) forms a V-shaped angle, with a shorter ventral side; the V-shaped articulatory fossa of the cardo is linked with the stipital base; the longer dorsal part of the cardinal apex reaches into the stipital base at an angle resulting in a very tight

articulation between both maxillary parts; the dorsal part of the cardinal apex is reinforced by transverse ridge (cdr, Fig. 5B); additionally it is connected with the stipes by a broad membranous band (cdm 5B); the surface of the cardo is largely smooth, but a longitudinal field of tooth-like denticles is present on its posterolateral side (Fig. 5B, box). The stipes (st, Figs. 5 and 6A, B) forms the main part of the maxilla; its outer surface is formed by the external stipital sclerite (Fig. 5B); a deep groove runs longitudinally on its mesal edge (stgl; Fig. 5) and transversely across the stipes at its distal end (stgt, Fig. 5). The transverse aspect of the groove receives the labrum when the maxillolabial complex is retracted, whereas the prementum interacts with the longitudinal aspect mesally; a sclerotized internal ridge is present laterally (stlr, Figs. 6B and 11D, E); the mesal margin of the external sclerite is broader than the lateral edge (Fig. 6A); the lateral margin is folded inwards distally and forms a broad, smooth distal surface (dlst, Fig. 6B) next to the palpus; the surface of the distal

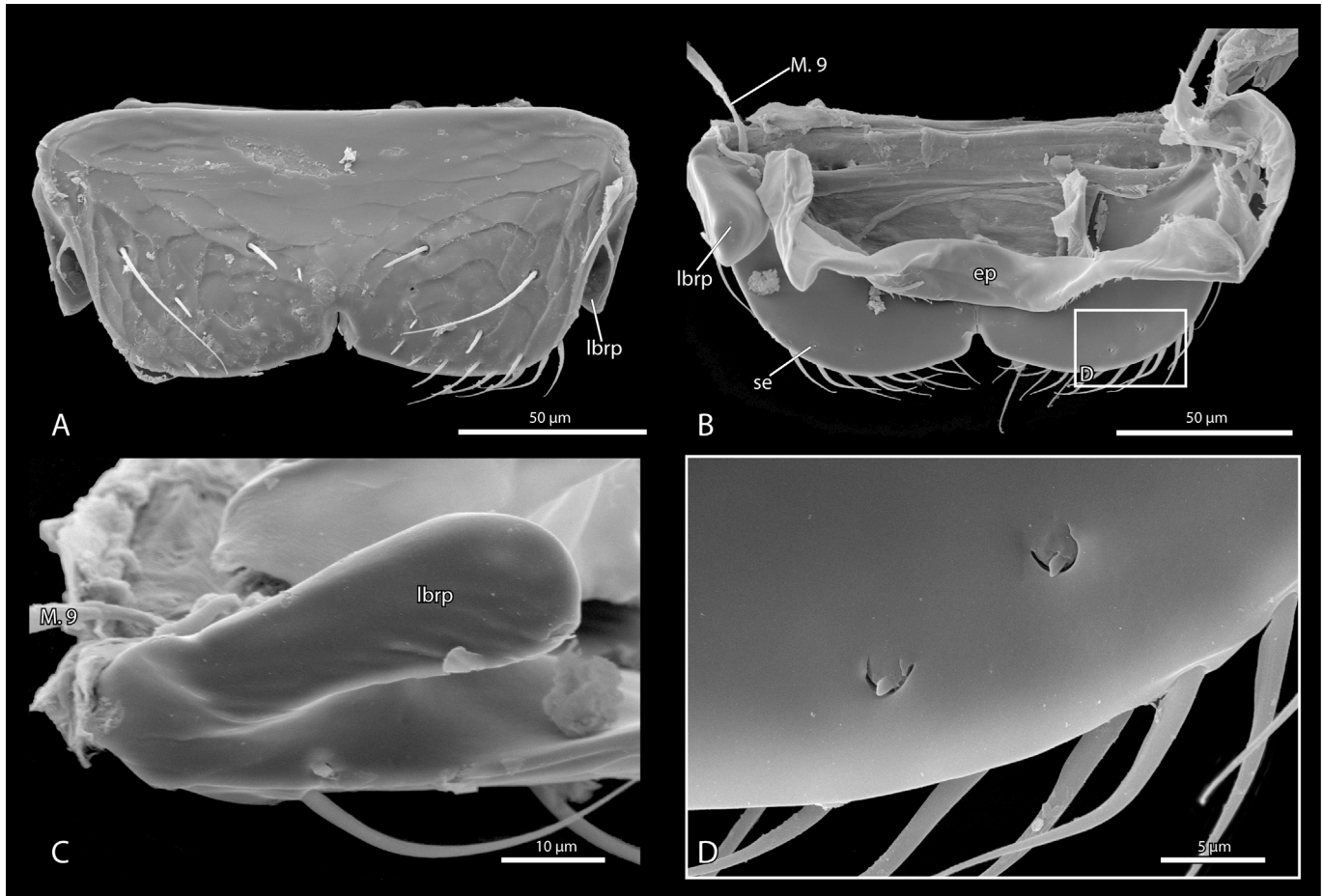


**Fig. 8.** SEM images of the labrum of *W. affinis*. **A.** Outer view. **B.** Inner view. **C.** Caudolateral view of a lateral process. **D.** Detail from B, sensilla on the inner distal surface. Abbreviations: **ep** — epipharynx, **M9** — *M. frontoepipharyngalis*, **se** — sensilla, **lbrp** — labral process.

region and the groove of the external stipital sclerite is smooth. The three-segmented maxillary palp (pmx, Figs. 5 and 6A, B) is inserted mesally on the distal stipital surface; palpomere 1 is flattened and subtriangular (Fig. 6B); segment 2 is approximately cylindrical but narrower proximally; palpomere 3 is slightly flattened and approximately oval. The closely connected galea and lacinia are linked to the mesal side of the stipes by a broad membranous zone and a stabilizing inner stipital sclerite (stps, Fig. 11F–H); both endite lobes are weakly sclerotized, but with increasing thickness of the cuticle on their dorsal side (section series); the galea is subrectangular and bent mesad above the labium in its resting position (Fig. 5B); the distal margin of the galea, the galeal crown, bears a row of setae of different length and partially with a blunt apex (gacr, Figs. 5 and 6A, B); the maxillary comb is formed by a dense row of setae on the inner (ventral) side along the free margin; most of them are stout and blunt, but those closer to the galeal crown are more pointed apically (mxc, Figs. 5 and 6A); aside from this structure, an additional row of distinctly thinner microtrichia is present on the galea (mtgl, Fig. 6E) and also some short, conical sensilla inserted in pores (csga, Fig. 6E); the lacinia appears also rectangular in lateral view, but its longer side forms an angle of 90° with the galea (lc, Fig. 6B); viewed from the internal side it appears subtriangular (Fig. 6A); at its free margin it bears a distinctly delimited lobe with a denticulate margin which bears a row of setae on its outer side (Fig. 6F); a proximad field of scale-like, strongly pectinate microtrichia is present on the inner side (Fig. 6C); distinctly separated scales with pectinate free margins are

present anteriorly, followed posteriorly by increasingly hair-like single microtrichia.

**Musculature (Figs. 9G–I, 11 and 12)** *M. craniocardinalis externus* (M. 15): well-developed muscle; O: postgena, anterad the concavity around the foramen occipitale; I: with a long and thin tendon on the lateral base of the cardo. *M. craniocardinalis internus* (M. 16): absent. *M. tentoriocardinalis* (M. 17): a slightly curved muscle; O anterior tentorial arm close to the anterior tentorial pit, additionally on the directly bordering head capsule; I: difficult to identify, probably on the membrane between cardo and stipes (section series). *M. tentoriostipitalis* (M.18): a flat, triangular muscle; O: ventral surface of the mesal lamella of the anterior tentorial arms; I: with two tendons, which merge with the base of the internal stipital sclerite. *M. craniolacinialis* (M. 19): absent. *M. stipitolacinialis* (M. 20): flat, small muscle; O: lateral stipital margin; I: distal internal stipital sclerite and base of the lacinia. *M. stipitogalealis* (M. 21); O: inner wall of the external stipital sclerite; I: with a short tendon on the inner base of the galea. *M. stipitopalpalis externus* (M. 22) or *M. stipitopalpalis internus* (M. 23): (not shown on the figure plates) thin muscle, difficult to identify in CT-scan. O: proximal inner wall of the external stipital sclerite lateral to M. 21. I: base of first palpomere. *M. palpopalpalis maxillae primus* (M. 24): (not shown on the figure plates) O: base of palpomere 1. I: base of palpomere 2. The other palp muscles are not clearly recognizable on the serial sections.

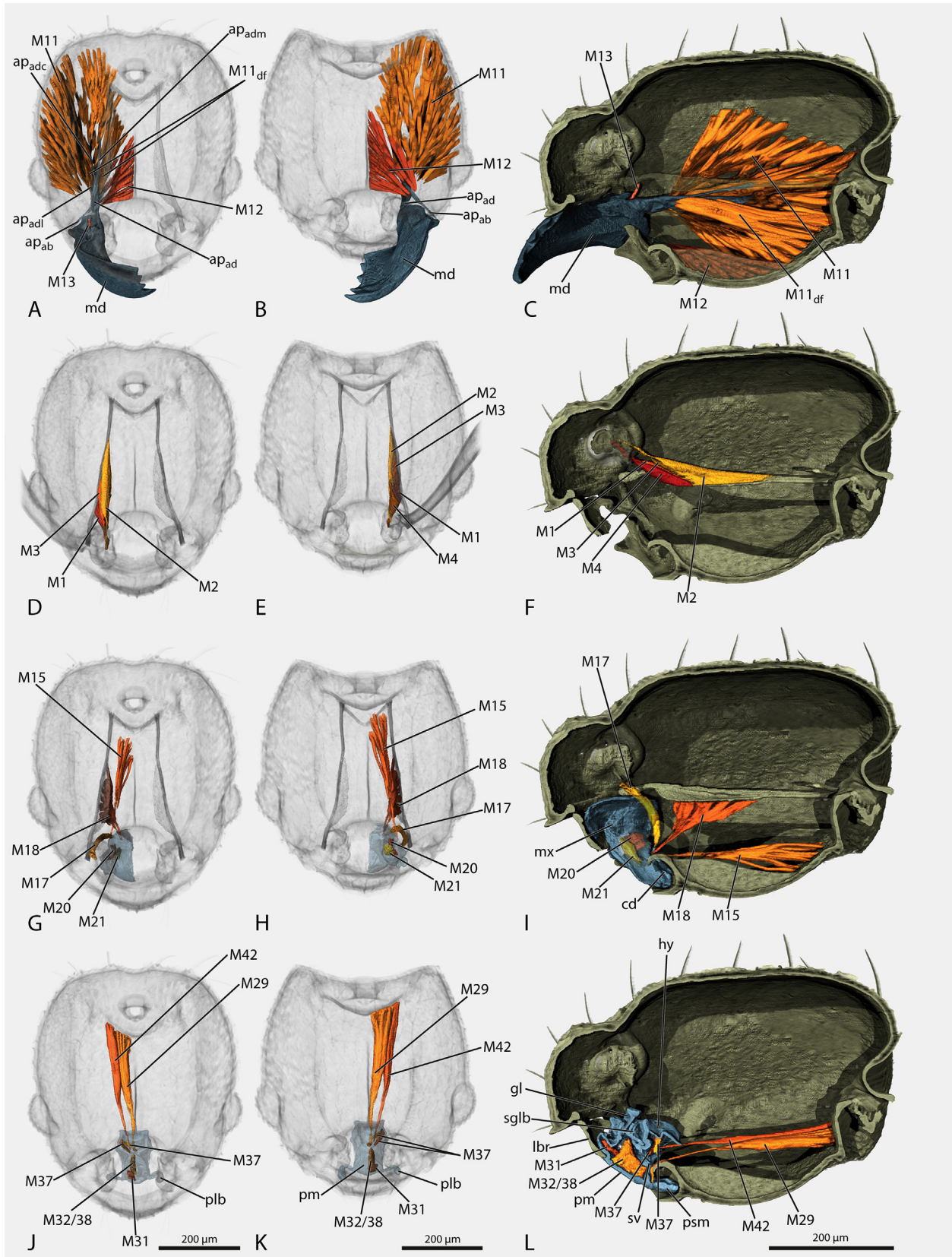


**Fig. 9.** 3D reconstructions of the musculature of the mouthparts and the antennae of *W. affinis*. Head capsule, labrum and endoskeleton are in grey, muscles are in red/orange and the maxillolabial complex including the labial part of the hypopharynx are in dark blue. **A–C.** Mandible. **D–F.** Antenna. **G–I.** Maxilla. **J–L.** Labium. **A, D, G, J.** Dorsal view. **B, E, H, K.** Ventral view. **C, F, I, L.** Sagittal view. Abbreviations: **ap<sub>ab</sub>** – apodeme of the mandible abductor, **ap<sub>ad</sub>** – apodeme of the mandible adductor, **ap<sub>adc</sub>** – central extension of the adductor apodeme, **ap<sub>adi</sub>** – lateral extension of the adductor apodeme, **ap<sub>adm</sub>** – medial extension of the adductor apodeme, **cd** – cardo, **gl** – glossa, **hy** – hypopharynx, **lbr** – labrum, **M1** – *M. tentorioscapalis anterior*, **M2** – *M. tentorioscapalis posterior*, **M3** – *M. tentorioscapalis lateralis*, **M4** – *M. tentorioscapalis medialis*, **M11** – *M. craniomandibularis*

### 3.6. Labium and distal hypopharynx

As part of the maxillolabial complex the labium is closely connected with the maxillae (Figs. 5A and 7) and also with the hypopharynx; its ventral surface is formed by the small postmentum (psm, Figs. 5A and 7B) and the distinctly larger prementum (Figs. 5A and 7G); the anterior upper surface is formed by the glossa (glo, Fig. 7A, G) and paraglossae (pgl, Fig. 7A, D, G, I), the posterior part by the hypopharynx (hy, Fig. 7A, G). The postmentum is a narrow, horseshoe-shaped sclerite; it is linked with the prementum by an extensive membranous area; the transitional area of sclerite and membrane displays a surface pattern with blunt denticles (Fig. 5A, box). The strongly sclerotized ventral side of the prementum forms a shield-like structure with a narrower proximal edge; the lateral premental margins (Fig. 11D, E) bear deep furrows (premental ditches) (pmd, Fig. 7G) where the mesal stipital margins fit into when the maxillolabial complex is retracted; proximally the furrows are confluent, thus separating the lower (ventral) premental surface (pmvs, Figs. 5A and 7G) from the lateral areas (pmls, Figs. 5A and 7G); additionally, a transverse groove is present on the ventral surface (pmtg, Figs. 5A and 7G), which forms a blunt angle and divides the prementum in a slightly larger rhomboid proximal region and a slightly shorter distal part (pmds, Figs. 5A and 7G); the distal edge of the labrum fits into this groove when the maxillolabial complex is retracted (Fig. 9L). The hypopharynx is formed by a nearly rectangular membranous complex elevated above the posterior half of the prementum (hy, Fig. 7A, G); it is stabilized by narrow premental arms arising proximally from the lateral margins of the prementum (pma, Figs. 7G and 12A); additionally it is mechanically reinforced by crescent-shaped sclerites (hysl, Fig. 11H), which are suspended at the premental arms and thickened anteriorly; moreover, the anterior hypopharynx is stabilized by sclerites (hypopharyngeal buttons), which anteroventrally merge with the salivary sclerite (hysd, Fig. 11H); the distalmost hypopharynx protrudes above the salivarium and the region between the subglossal brushes (Figs. 7G and 11G); the concave anterolateral margins of the hypopharynx bear some cuticular denticles (Fig. 7K); the median part of the tongue-like structure is covered by hair-shaped microtrichia, which are arranged as short combs; similar structures are also present on the dorsal hypopharyngeal surface (Fig. 7E, J); posteriorly they are increasingly shaped like apically pectinate cuticular scales (Fig. 7F); the anterior region of the hypopharynx forms a smooth groove medially (hyg, Fig. 7A); the hypopharynx posteriorly extends into the infrabuccal pouch (ibp, Fig. 10F); it also forms the ventral wall of the buccal tube (bt, Fig. 10F) and remaining prepharynx, with the sitophore plate as distinctly sclerotized element (sp, Figs. 10F and 11B–G). The two-segmented labial palps (plb, Figs. 5A and 7A, G) insert distally in marginal premental furrows; palpomere 1 is flattened and appears slightly twisted; the club-shaped segment 2 is inserted on the flat anterior side of palpomere 1; setae are inserted on its dorsal, lateral and distal surface, but specific types of sensilla could not be identified with the applied techniques. The glossa is dorsally inserted in the distal membranous area of the prementum; it is stabilized by a small, elongate ventral glossal sclerite (glvs, Fig. 11C) at its ventral base and by the larger paired dorsal glossal sclerites (glds, Fig. 11C–E) dorsolaterally; these sclerites are connected with the lower salivarium by ligamentous structures or continuous with it; additionally, ventrolateral basiglossal arms are present as anterior extensions; its anteromedian margin is rounded and smooth and

ends in parallel-sided cuticular stripes with truncate apical edges (Fig. 7B); the remaining part of the glossa, the dorsal surface, is membranous. The glossa of the available specimens was strongly folded, probably as an artefact of the preparation (Fig. 7A, G); the surface of the glossa is covered with rectangular plate-like structures (Fig. 7C), which overlap in a scale-like manner, especially close to the glossal margins; the scales closest to the margin are elongated posteriorly, which results in an obliquely elongated distal margin (Fig. 7H); the anterior edges are rounded whereas the posterior ones are acutely prolonged; some of the scales are narrow and resembling microtrichia. The paraglossae are present as distinctly reduced membranous lobe-like structures laterad the glossa; distally they are extended as flat, elongate and parallel-sided cuticular stripes which converge medially (Fig. 7D, I); posteriorly the paraglossae are connected with the bases of the subglossal brushes (sglb, Figs. 7A, G, 11E, F); these structures behind the main part of the glossa are composed of stout, apically blunt, almost club-shaped setae arranged on flat plates; laterad these setae distally pectinate flat cuticular scales are arranged in five to eight rows; they are similar to the scales on the hypopharynx and on the inner area of the lacinia.

**Musculature (Figs. 9J–L, 11 and 12):** *M. tentoriopraementalis inferior* (M. 29), O: posterior postgena below the tentorial bridge, mesad M. 42; I: the tendons of the paired muscle unite medially as a broad unpaired structure which extends over the tip of the postgena and inserts on the posterior premental margin. *M. praementoparaglossalis* (M. 31), O: approximately on half length of the lateral surface of the prementum; I: mostly on the ventral glossal sclerite, probably also on the anterior prementum. *M. praementoglossalis* (M. 32), well developed muscle, O: middle region of the ventral surface of the prementum; I: dorsal glossal sclerites and below the salivarium; difficult to separate from M. 38/39, especially with  $\mu$ CT-data. *M. praementopalpalis externus* (M. 34), not clearly recognizable, apparently difficult to separate from M. 31. *M. palpalpalis labii* (M. 35/36), not distinctly recognizable in the available data sets, but at least M. 35 is apparently present. *M. tentoriohypopharyngalis* (M42), O: posterior postgena below the posterior tentorial pit, laterad M. 29; I: distal sclerite of the hypopharynx/salivary sclerite (both probably merged, s. salivarium).

### 3.7. Salivarium

The salivary duct (sald, Fig. 12B) opens at the labiohypopharyngeal connecting area at the base of the hypopharyngeal protrusion posterior and between the subglossal brushes; the opening is mainly sclerotized on its dorsal side (sv, Figs. 11F–H and 12B); a U-shaped sclerotized fold is present below the duct, originating between the subglossal brushes (Fig. 12B); additionally, the distal salivarium is linked with the distal sclerites of the hypopharynx, the hypopharyngeal button (hysd, Fig. 11H); the U-shaped fold obliterates posterior to the labium and the ductus salivarialis (sald, Fig. 12B) continues as simple thin tube into the thorax, where it connects with the salivary glands.

**Musculature (Figs. 9J–L, 11 and 12A):** *M. hypopharyngosalivarialis* (M. 37), appears like two closely adjacent bundles, O: dorsolaterad from the lateral crescent-shaped sclerite of the hypopharynx; I: dorsolaterally on the ductus salivarialis and on the ventral side of the salivary sclerite and duct. *M. praementosalivarialis anterior & (or) posterior* (M. 38, 39), O: on the proximal side of the prementum; I: on the lower

*internus*, **M11<sub>dr</sub>** — directly attaching fibers of M11, **M12** — *M. craniomandibularis externus*, **M13** — *M. hypopharyngomandibularis*, **M15** — *M. craniocardinalis externus*, **M17** — *M. tentoriocardinalis*, **M18** — *M. tentoriostipitalis*, **M20** — *M. stipitolacinalis*, **M21** — *M. stipitogaealis*, **M29** — *M. tentoriopraementalis inferior*, **M31** — *M. praementoparaglossalis*, **M32/38** — *M. praementoglossalis* and *M. praementosalivarialis*, **M37** — *M. hypopharyngosalivarialis*, **M42** — *M. tentoriohypopharyngalis*, **md** — mandible, **mx** — maxilla, **plb** — labial palp, **pm** — prementum, **psm** — postmentum, **sglb** — subglossal brush.

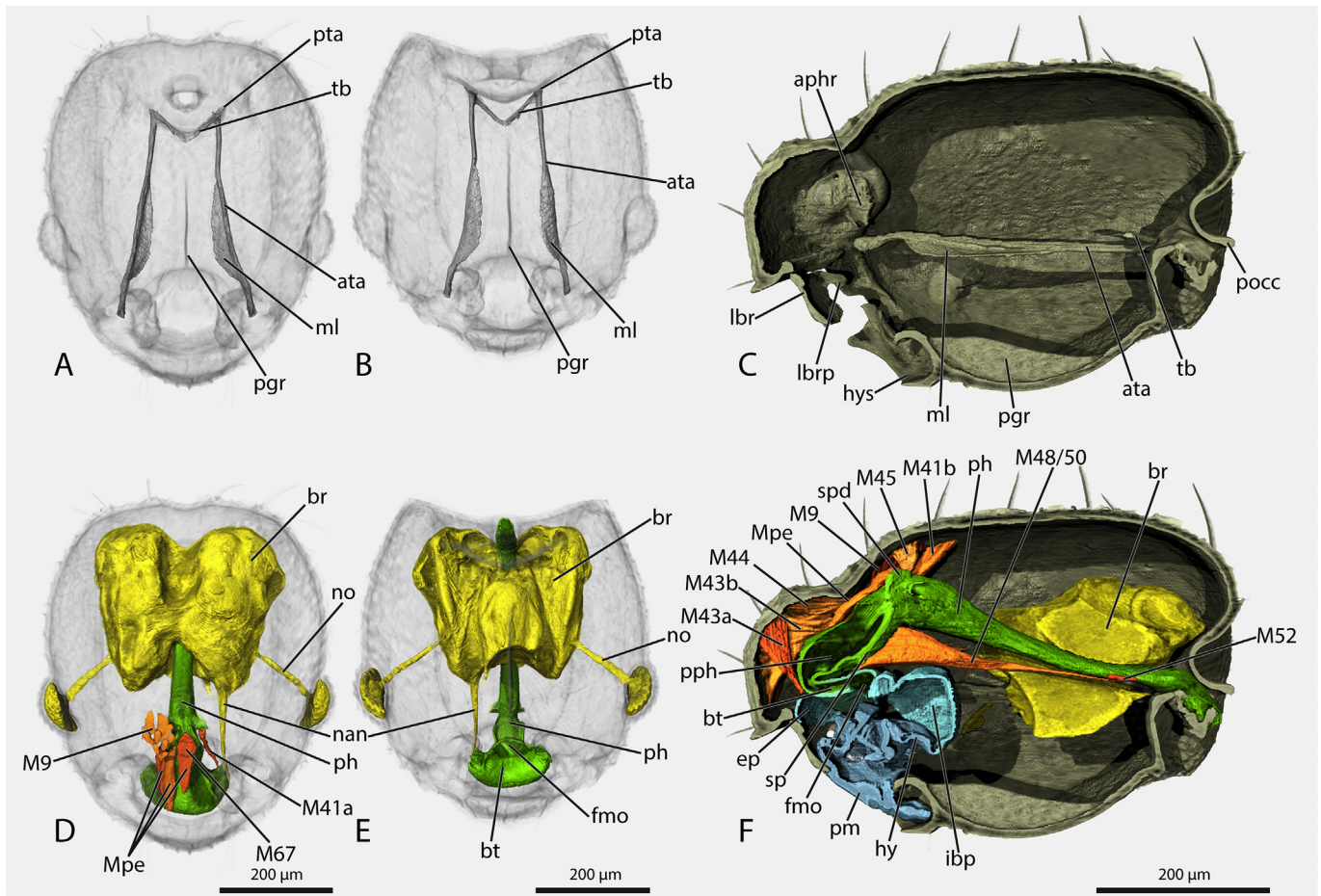


**Fig. 10.** 3D reconstructions of the head of *W. affinis*. Head capsule, labrum and endoskeleton are in grey, muscles are in red/orange, digestive tract is in green, the free part of the epipharynx and the infrabuccal pouch are in light blue, the maxillolabial complex including the labial part of the hypopharynx are in dark blue and the nervous system is in yellow. **A.** Tentorium dorsal view. **B.** Tentorium ventral view. **C.** Head skeleton in sagittal view. **D.** Brain, digestive tract, longitudinal muscles of the prepharynx and labrum in dorsal view. **E.** Digestive tract and brain in ventral view. **F.** Brain, digestive tract in association with the labium and muscles of the prepharynx and pharynx in sagittal view. Abbreviations: **ata** – anterior tentorial arm, **aphr** – phragma at the antennal insertion, **br** – brain, **bt** – buccal tube, **ep** – epipharynx, **fmo** – functional mouth opening, **hy** – hypopharynx, **hys** – hypostoma, **ibp** – infrabuccal pouch, **lbr** – labrum, **lbrp** – labral process, **ml** – median lamella of the anterior tentorial arm, **M9** – *M. frontoepipharyngealis*, **M41a** – *M. frontohypopharyngealis*, lateral aspect, **M41b** – *M. frontohypopharyngealis*, dorsal aspect, **M43a** – *M. clypeopalatalis*, portion of buccal tube, **M43b** – *M. clypeopalatalis*, portion of anterior prepharynx, **M44** – *M. clypeobuccalis*, **M45** – *M. frontobuccalis anterior*, **M48/M50** – *M. tentoriobuccalis anterior/posterior*, **M52** – *M. tentoriopharyngealis*, **M67** – *M. transversalis buccae*, **Mpe** – *M. pharyngoepipharyngealis*, **nan** – antennal nerve, **no** – optic nerve, **pgr** – postgenal ridge, **ph** – pharynx, **pm** – prementum, **pocc** – postocciput, **pph** – prepharynx, **pta** – posterior tentorial arm, **sp** – sitophore plate, **spd** – dorsal process of the sitophore plate, **tb** – tentorial bridge.

sclerotized area of the salivarium; very difficult to separate from M. 32, especially in the  $\mu$ -CT-data set, possibly fused to it.

### 3.8. Labrum

The trapezoid sclerotized labrum is movably attached to the infolded distal clypeal margin (Figs. 8 and 10C); it is distinctly bilobed with a median notch at its distal margin (Fig. 8A, B); lateral labral arms are present as posteriorly directed processes at the posterolateral edges of the labrum (lbrp, Figs. 8B, C and 10C). When the mouthparts are retracted the distal corners of the stipites overtop the labral arms, while the distal margin of the labrum also articulates with the transverse grooves of the prementum (Fig. 9L) and stipites; the preoral space is efficiently sealed off by this interlocking mechanism that closely fits the sclerites of the labrum, prementum and stipites.

**Musculature** (Figs. 10D, 11 and 12): *M. frontoepipharyngealis* (M. 9), O: inner surface of the frontal area posterad the antennal bases; I: with a thin, long tendon (not recognizable in 3D

reconstruction) proximally on the labrum, proximad the lateral labral arms.

### 3.9. Epipharynx

The anteriormost epipharyngeal part is the unsclerotized inner wall of the labrum. The main part of the epipharynx (ep, Figs. 8B and 10F) forms the semimembranous upper wall of the laterally open buccal cavity, and also the roof of the prepharynx including the buccal tube, which bears distinct bulges on the anterior part of its lateral wall (Fig. 11B–F). The prepharynx is formed by the fusion of the lateral edge of the posterior epipharynx with the corresponding edge of the posterior hypopharynx. The cuticular surface of the epipharynx is largely smooth, but rows of minute microtrichia are present, especially in the region of the buccal tube.

**Musculature** (Figs. 10D, F and 11): *M. clypeopalatalis* (M. 43) strongly developed, two distinct subcomponents: M43a: unpaired O: medially on the clypeus; I: on the transition area between the epipharynx and buccal tube. M43b: paired O: anterolateral and

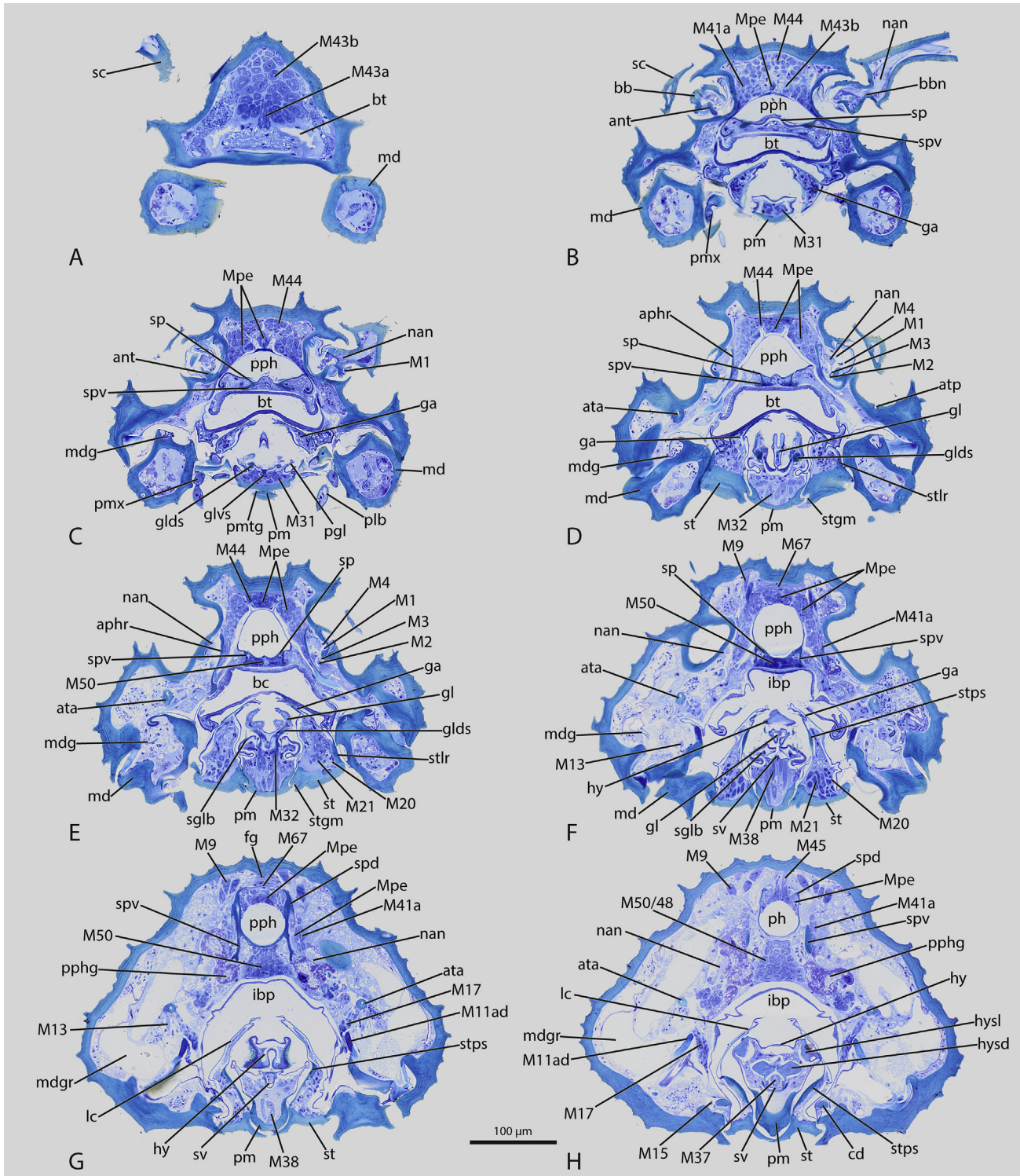


**Fig. 11.** Photomicrographs of cross sections through the head of *W. affinis*. From **A–H** continuously further back in the head capsule. Abbreviations: **ant** — antennifer, **aphr** — phragma at the antennal insertion, **ata** — anterior tentorial arm, **atp** — anterior tentorial pit, **bb** — bulbus of the scape, **bbn** — bulbus neck, **bc** — buccal cavity, **bt** — buccal tube, **cd** — cardo, **fg** — frontal ganglion, **ga** — galea, **gl** — glossa, **glds** — dorsal glossal sclerite, **glvs** — ventral glossal sclerite, **hy** — hypopharynx, **hysd** — distal hypopharyngeal sclerite, **hysl** — lateral hypopharyngeal sclerite, **lc** — lacinia, **M1** — *M. tentorioscapalis anterior*, **M2** — *M. tentorioscapalis posterior*, **M3** — *M. tentorioscapalis lateralis*, **M4** — *M. tentorioscapalis medialis*, **M9** — *M. frontoepipharyngalis*, **M11<sub>ad</sub>** — apodeme of M11, **M13** — *M. hypopharyngo-mandibularis*, **M15** — *M. craniocardinalis externus*, **M17** — *M. tentoriocardinalis*, **M20** — *M. stiptolacinalis*, **M21** — *M. stiptogalealis*, **M31** — *M. praementoparaglossalis*, **M32** — *M. praementoglossalis*, **M37** — *M. hypopharyngosalivarialis*, **M38** — *M. praementosalivarialis*, **M41a** — *M. frontohypopharyngealis*, lateral aspect, **M43a** — *M. clypeopalatalis*, portion of buccal tube, **M43b** — *M. clypeopalatalis*, portion of anterior prepharynx, **M44** — *M. clypeobuccalis*, **M45** — *M. frontobuccalis anterior*, **M48/50** — *M. tentoriobuccalis anterior/posterior*, **M67** — *M. transversalis buccae*, **Mpe** — *M. pharyngoepipharyngealis*, **md** — mandible, **mdg** — duct of the mandibular gland, **mdgr** — mandibular gland reservoir, **nan** — antennal nerve, **pgl** — paraglossa, **plb** — palpus labialis, **pm** — prementum, **pmx** — palpus maxillaris, **pmtg** — transverse premental groove, **pph** — prepharynx, **sc** — scape, **sglb** — subglossal brush, **sp** — sitophore plate, **spd** — sitophore plate dorsal process, **spv** — sitophore plate ventral process, **st** — stipes, **stgl** — stipital groove, longitudinal aspect, **stgm** — mesal stipital groove, **stlr** — lateral stipital ridge, **sv** — salivarium.

central surface of clypeus. I: dorsal prepharynx at about the level of the insertion of the median longitudinal muscle. **M. clypeobuccalis (M. 44)**, strongly developed, O: posteriorly on the convex part of the clypeus. I: at the level of the anatomical mouth opening. **M. pharyngoepipharyngealis (Mpe)**: Longitudinal muscles connecting the anterior pharynx and the epipharynx: very strongly developed, paired lateral and unpaired median longitudinal muscle strands on the dorsal side of the prepharynx between the insertion sites of M. 43b and M. 45; the lateralmost bundle inserts on the posterior phragma of the ventral process of the sitophore plate.

### 3.10. Cephalic digestive tract

The anteriormost pharyngeal section is slightly oval in cross section, whereas the main part of the pharynx is approximately cylindrical (ph, Figs. 10D–F, 11H and 12); anteriorly the pharynx is continuous with the broader prepharynx. The border between the pharynx and the prepharynx is the anatomical mouth opening, which is generally marked by the frontal ganglion (fg, Fig. 11G) and the insertion of M. 45 (M45, Fig. 11H). The prepharynx has a wider lumen (pph, Figs. 10D–F and 11B–G) than the pharynx; the anteriormost pharyngeal section and the prepharynx are distinctly bent downwards and run nearly parallel to the dorsal wall of the head capsule (Fig. 10F); anteriorly the prepharynx is abruptly bent posteroventrad and forms the broad buccal tube (bt, Figs. 10D–F and 11B–D), which appears approximately U-shaped in cross section; due to its curvature it nearly runs in opposite direction to the remaining prepharyngeal section; distally the tube opens broadly at the functional mouth opening (fmo, Fig. 10D–F) and is continuous with the laterally open buccal cavity (bc, Fig. 11E). The cuticle of the buccal tube is thick, especially on the anterior side, and it bears fine posteriorly/ventrally oriented microtrichia; the distal lip of the anterior side, which bears a vestiture of long microtrichia, is continuous with the semimembranous part of the epipharynx (ep, Fig. 10F) forming the roof of the buccal cavity; the posterior wall of the buccal tube is continuous with the infrabuccal pouch (ibp, Figs. 10F, 11F–D and 12A–C), but a fold is recognizable in the transition area. The ventral wall of the prepharynx is strongly sclerotized posterad the curvature, thus forming a sitophore plate (sp, Figs. 10F and 11B–G); this structure bears a pair of longitudinal sclerotized processes, which have a different orientation at different levels; anteriorly they are directed ventrad and reach from the anterior section of the prepharynx to the level of the antennal insertions (spv, Fig. 11B–H); proximally the ventral processes are bent laterad thus stabilizing the posterior wall of the buccal tube (Fig. 11B–E); further posterad they are straight and elongated; towards the end of the ventral processes, the sitophore plate extends increasingly over the lateral prepharyngeal wall; at the level of the anatomical mouth opening it forms dorsal processes which fuse with the ventral processes in the prepharyngeal wall, the processes are extended as short phragmata in this region (Fig. 11H); the dorsal processes (spd, Figs. 11G, H and 12A) extend posterad over a short distance of the pharynx, and are continuous with short lateral processes on the level of the openings of the pharyngeal glands (spl, Fig. 12B) (the processes of the sitophore plate are also referred to as oral arms). The oesophagus is continuous with the posterior pharynx with the border approximately marked by the position of the tentorial bridge; aside from the lack of a layer of ring muscles it does not differ from the pharynx.

**Musculature (Figs. 10D, F, 11 and 12): M. frontohypopharyngealis (M. 41)**, two very distinct subunits; anterior subunit (M. 41a), O: phragma of the acetabulum of the antennal insertion. I: lateral processes of the sitophore plate at the level of the pharyngeal gland opening; posterior subunit (M. 41b), O: frontal area, posterad the origin of M. 46; I: on the lateral dorsal processes of the

sitophore plate at the level of the openings of the pharyngeal glands. **M. frontobuccalis anterior (M. 45)**, rather weakly developed, closely adjacent along midline, thus appearing unpaired, O: on the inner surface of the frontal area, directly posterad the frontoclypeal sulcus; I: medially on the dorsal side of the pharynx, posterior to the frontal ganglion (Fig. 11G). **M. frontobuccalis posterior (M. 46)**, weakly developed (not visible in 3D-reconstructions), O: on the frontal area, directly posterad M. 45; I dorsomedially on the pharynx posterad M. 45, approximately on the level of the insertion of (M. 41) (Fig. 12B). **M. tentoriobuccalis anterior/posterior (M. 48/M. 50)**, strongly developed muscle, O: on the anterior process of the tentorial bridge with a long tendon. I: ventrally on the sitophore plate, between its ventral processes. **M. tentoriopharyngalis (M. 52)** (Fig. 10F), a very small muscle, O: tentorial bridge laterad M 48/50; I: ventral side of pharynx at the level of the suboesophageal ganglion. **M. transversalis buccae (M. 67)**, a layer of transverse muscles between the dorsal processes of the sitophore plate, anterior to the frontal ganglion (Fig. 11F, G) and anterior to an additional layer of transverse muscles on the ventral side of the pharynx at the level of M. 45. **M. annularis stomadaei (M. 68)**, a thin layer of ring muscles around the pharynx from the area of the openings of the pharyngeal glands to the region of the tentorial bridge. **M. longitudinalis stomadaei (M. 69)**, weakly developed layer of longitudinal muscles below the ring musculature of the pharynx.

### 3.11. Cephalic glands

Several glands are present in the head. The mandibular glands open via sclerotized ducts (mdg, Fig. 11C–F) on the mandibular base at the mandalus. Large reservoirs are present proximad these channels in the ventral region of the head capsule (mdgr, Fig. 11G, H). Gland tissue in the lumen of the mandibles, especially in the ventral region (Fig. 11A–E), forms the intramandibular gland. Maxillary glands were absent in the examined specimens. The very large prepharyngeal glands (pphg, Figs. 11G, H and 12A–D) (“propharyngeal glands”; Boonen and Billen, 2016) are placed above the infrabuccal pouch and overreach it distinctly posteriorly; the anterior part of the assemblage of gland cells is medially divided by the large M. 48/50. The large pharyngeal glands (phg Fig. 12B–G) (“postpharyngeal glands”; Boonen and Billen, 2016) open laterally into the pharynx (phgo, Fig. 12B) a short distance posterad the anatomical mouth opening; voluminous reservoirs are present in this region and divide into several elongated sacs; they almost reach the region of the tentorial bridge and decrease in width posteriorly.

### 3.12. Brain and suboesophageal complex

The brain (br, Figs. 10D–F and 12E–H) forms a compact structural unit with the suboesophageal complex, with a narrow central passage for the pharynx; it is voluminous in relation to the size of the head capsule (brW/hW = 0,65); in dorsal view it appears trapezoidal with rounded edges and deep folds on the anterior, posterodorsal and posterior side; it is located posterad the compound eyes on the level of the foramen occipitale; the mushroom bodies are very large and the olfactory lobes are also well-developed; in contrast, the optic lobes are very small compared to the brain size. The optic neuropils are thin; the lamina is hardly visible and located within the long optical nerve; medulla and lobula are small neuropils in the lateral brain, basal to the optical nerve; the thin optical nerves (no, Fig. 10D, E) originate on the anterior side of the protocerebrum and run obliquely towards the compound eyes between fibers of M. 11. The antennal nerves originate on the anterior tips of the deutocerebral subunits of the

brain (nan, Figs. 10D, E, 11CeH and 12A, D); they run nearly straight anterad and enter the scapus.

### 3.13. Fat body

Fat body cells are loosely arranged between other internal structures of the head, they are also present in the lumen of the labrum, mandibles and maxillae.

### 3.14. Tracheae

Two pairs of large trachea entering the head capsule are strongly narrowed in the region of the occipital foramen (tra, Fig. 12G). The dorsal main tubes widen strongly in the cephalic lumen; a large branch enters the posterior part of the head capsule and additional paired branches extend into the ventrolateral regions, where they mainly run between fibers of M. 11; anteriorly they are closely adjacent with the lateral side of the brain. The paired ventral tracheae split into two branches shortly after entering the cephalic lumen; the mesal branches run along the sides of the pharynx, whereas the external ones extend towards the anterior head region below the anterior tentorial arms. Many smaller branches originating from the larger ones supply the organs of the head.

## 4. Discussion

### 4.1. Standardized anatomical investigation of Formicidae

Despite extensive morphological data in several phylogenetic and morphological studies, the available anatomical data on the head of Formicidae are fragmentary. In the present contribution we suggest a standardized morphological treatment of body regions or tagmata of ants to increase the inventory of morphological data for the group, providing detailed and well-documented morphological data sets. This can help to resolve persisting phylogenetic problems and especially help to properly place fossil taxa within a phylogenetic framework. More importantly, it will allow tracing character evolution in detail, consequently allowing the identification of key phenotypic changes through the formicid phylogeny and their evolutionary and ecological consequences. A first example of this was presented in a study on the mesosoma of *Myrmecia nigrocincta* Smith, F., 1858, which employed similar methods to those used here (Liu et al., 2019, in press).

The procedure applied here is even suitable if only a minimum of specimens or even a single one is available, although several specimens as used here allow for the use of more techniques and ultimately yield a more complete morphological data set. A first step is the documentation of the external surface with microphotography (e.g. Wipfler et al., 2016; also used extensively on [antweb.org](http://antweb.org)). This is suitable for recording the colouration and sculpture of the cuticle, and with some limitation also the degree of sclerotization, with strongly sclerotized areas often darkened and semi-membranous or membranous areas usually depigmented and whitish. Specimens dried at critical point can be used for SEM micrographs, with a rotatable specimen holder (Pohl, 2010) to obtain all standard views from a single specimen, always with a homogenous black background and minimum charging effects. The same dried specimen can also be used for  $\mu$ -computed tomography ( $\mu$ CT), providing perfectly aligned image stacks suitable for computer-based anatomical 3D reconstruction. While  $\mu$ CT produces perfect datasets for 3D reconstruction, some features such as gland tissue and muscle striation as well as the tracheal system (although see Webster et al. (2015) for a discussion of possible artifacts caused by this method) can be better investigated using histological sections. Finally, the stepwise re-soaking of the

specimen with an ethanol series of increasing concentration allows serial sectioning. The use of Araldite as embedding medium and diamond knives yield section series of a thickness of 0.5–1 mm of high quality. An additional method suitable for small or very small and transparent specimens is confocal laser scanning microscopy (CLSM) (Wipfler et al., 2016). This was for example successfully applied in a study on the maxillolabial complex of *Sparasion* (Hymenoptera, Platygastroidea) (Popovici et al., 2014). The potential of this technique for anatomical studies on ants should be further explored in the future. To obtain detailed data on the mouthparts, especially the maxillolabial complex, it is advisable to dissect them and separate maxillae and labium from each other. Otherwise not all potentially interesting characters can be documented. At least two specimens are required for this approach, however, and dissection can be a great challenge if the studied species is small. In the present study, a multitude of worker specimens had to be used as the small size of *W. affinis* (Head length ca. 650  $\mu$ m) made preparations very challenging and several specimens were needed to get useable samples of all the different structures.

A standardized and detailed documentation of external and internal structures of the head as well as other characters in Formicidae (and other groups of Hymenoptera) appears highly desirable and could be rewarding in light of the rather scattered documentation presently available in the literature. Many structures, especially the ones difficult to access, are not yet documented in enough detail to allow phylogenetic or evolutionary inferences based on them. Examples of potentially interesting characters not yet documented in detail are the distal hypopharynx with the hypopharyngeal groove, the prepharynx and its cuticular extensions, the musculature especially of the pharynx and prepharynx, the endoskeleton, especially the tentorium, the inner side of the lacinia, the surface structure of the glossa and the mandibular articulation.

### 4.2. Homology problems

The terminology used in both older and contemporary studies on ant anatomy is only partly compatible with the general standard in entomology (e.g. Snodgrass, 1935; Beutel et al., 2014). This is especially so for the interpretation of structures of the cranial digestive system, which differs from that in studies on other groups of insects, including non-formicid groups of Hymenoptera (Vilhelmsen, 1996; Beutel and Vilhelmsen, 2007; Zimmermann and Vilhelmsen, 2016). What is designated as anterior pharynx or just pharynx in anatomical studies on ants (e.g. Forbes, 1938, Whelden, 1957a,b; Peregrine et al., 1973, Hansen et al., 1999), is clearly identified as prepharynx here, based on the position of the frontal ganglion and the insertion of *M. frontopharyngalis anterior* (M45) and *M. frontohypopharyngalis* (M41), constant landmarks indicating the prepharyngeal-pharyngeal border. In contrast to the pharynx, the prepharynx is usually shaped like a transverse crescent or a flattened U in cross section, with its dorsal and ventral walls formed by the more or less sclerotized posterior epi- and hypopharynx, respectively. In the investigated ants the region of the “buccal tube”, actually a strongly bent anterior part of the prepharynx, is U-shaped, while the remaining prepharynx is more crescent-shaped to transversely oval. The buccal tube was previously interpreted as part of the pharynx (e.g. Hansen et al., 1999). The region designated as posterior pharynx in studies on Formicidae (such as Peregrine et al., 1973) is consequently the precerebral pharynx followed by the postcerebral pharynx, which is posteriorly continuous with the oesophagus. The pharynx can be distinguished from the prepharynx by a very thin intima, a layer of ring muscles, and longitudinal folds for attachment of dilators (e.g. Beutel and Vilhelmsen, 2007), usually dorsolaterally, laterally, and ventrolaterally, although such folds are missing in the studied ant

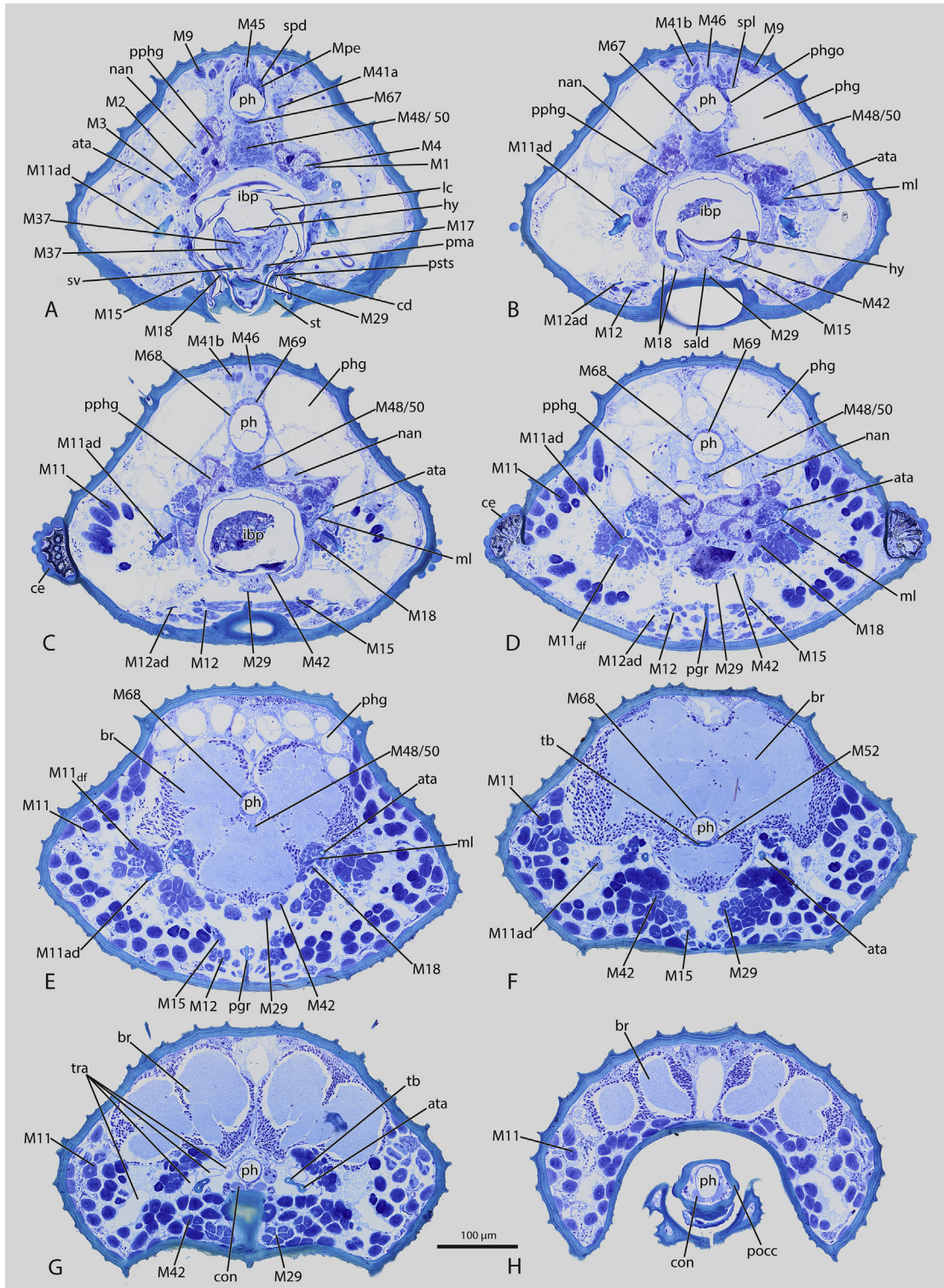


**Fig. 12.** Photomicrographs of cross sections through the head of *W. affinis*. From **A-H** continuously further back in the head capsule. Abbreviations: **ata** — anterior tentorial arm, **br** — brain, **cd** — cardo, **ce** — compound eye, **con** — connective, **hy** — hypopharynx, **ibp** — infrabuccal pouch, **lc** — lacinia, **M1** — *M. tentorioscapalis anterior*, **M2** — *M. tentorioscapalis posterior*, **M3** — *M. tentorioscapalis lateralis*, **M4** — *M. tentorioscapalis medialis*, **M9** — *M. frontoepipharyngalis*, **M11** — *M. craniomandibularis internus*, **M11<sub>ad</sub>** — apodeme of M11, **M11<sub>df</sub>** — M11, direct fibre, **M12** — *M. craniomandibularis externus*, **M12<sub>ad</sub>** — apodeme of M12, **M15** — *M. craniocardinalis externus*, **M17** — *M. tentoriocardinalis*, **M18** — *M. tentoriostipitalis*, **M29** — *M. tentoriopraementalis inferior*, **M37** — *M. hypopharyngosalivarialis*, **M41a** — *M. frontohypopharyngealis*, lateral aspect, **M41b** — *M. frontohypopharyngealis*, dorsal aspect, **M42** — *M. tentoriohypopharyngealis*, **M45** — *M. frontobuccalis anterior*, **M46** — *M. frontobuccalis posterior*, **M48/50** — *M. tentoriobuccalis anterior/posterior*, **M52** — *M. tentoriopharyngalis*, **M67** — *M. transversalis buccae*, **M68** — *M. anularis stomodaei*, **M69** — *M. longitudinalis stomodaei*, **Mpe** — *M. pharyngoepipharyngealis*, **ml** — median lamella of the tentorium, **nan** — nervus antennalis, **pgr** — postgenal ridge, **ph** — pharynx, **phg** — pharyngeal gland, **pma** — premental arm, **pocc** — postociput, **pphg** — prepharyngeal gland, **phgo** — opening of the pharyngeal gland into the pharynx, **psts** — internal stipital sclerite, **sald** — salivarial duct, **spd** — sitophore plate dorsal process, **spl** — lateral process of sitophore plate, **st** — stipes, **sv** — salivarium, **tb** — tentorial bridge, **tra** — tracheae.

species and apparently also other aculeates (Duncan, 1939), most likely in connection with the reduction of pharyngeal dilators (see Table 1). The re-interpretation of the foregut implies that the “propharyngeal glands” (e.g. Boonen and Billen, 2016) should be addressed as prepharyngeal glands, and the “postpharyngeal glands” (e.g. Peregrine et al., 1973; Schoeters and Billen, 1996) as pharyngeal glands (see Results).

The “infrabuccal sac” is commonly listed among the autapomorphies of Formicidae (e.g. Bolton, 2003; Boudinot, 2015). The common positional description “between labium and hypopharynx” would describe the space around the opening of the salivarium below the overhanging distal tip of the hypopharynx. However, Bolton’s (2003) description of this sac as “containing particulate matter, usually derived from food” indicates that he is referring to the infrabuccal pouch, which is part of the hypopharynx instead of the space between it and the labium. In any case this character would not represent an autapomorphy of Formicidae. A distal hypopharynx overhanging parts of the labium/salivarium also occurs in other groups of Aculeata (see e.g. Duncan, 1939), and the infrabuccal pouch is an autapomorphy of the entire Hymenoptera (Beutel and Vilhelmsen, 2007).

Other terms only used in myrmecology are mandalus, trulleum and canthellus, all of them referring to structures at the base of the mandibles, apparently without homologues in other groups of Hymenoptera (see also e.g. Hermann et al., 1971). In fact, a trulleum only occurs in a subset of Myrmecinae as a structure delimited by the canthellus and the structure identified as trulleum in Gotwald (1969) is actually the secondary mandibular articulation surface in most ant species. This mistake has been repeated in other studies (such as Brandão et al., 2010). The misdesignation of a structure that is not present seriously hampers the understanding of the basal mandibular area confounding a very important structure in the secondary mandibular articulation. This is one possible reason that this structure has received comparatively little focus in previous studies.

A conspicuous labial structure is the subglossal brush. Brushes of setae in this position also occur in other hymenopterans and are usually designated as basiparaglossal brush (Popovici et al., 2014; Hymenoptera Anatomy Ontology: [http://purl.obolibrary.org/obo/HAO\\_0002199](http://purl.obolibrary.org/obo/HAO_0002199)) or paraglossal sclerites together with their cuticular base (e.g. Cowley, 1959). As the paraglossae are usually strongly reduced in ants, the potential homology of the subglossal brush with a paraglossal structure has been previously neglected in the ant literature.

#### 4.3. Character evolution

Despite of a high degree of specialization, Formicidae maintain a number of groundplan features of Hymenoptera. Among them are the concave shape of the occipital region - obviously not affected by the prognathism – the absence of frontal ecdysial lines (Beutel and Vilhelmsen, 2007) (although note that median lines are visible in many ant species, possibly derived from the coronal suture, [B. Boudinot pers. obs.]), the inflected clypeus (Vilhelmsen, 1996, e.g. Fig. 10C), the maxillolabial complex (Beutel et al., 2008, Fig. 5A), the sitophore plate (sp, Fig. 11), the infrabuccal pouch (ibp, Figs. 10F, 11 and 12), and strongly developed longitudinal epipharyngeal muscles (Mpe, Figs. 10D and 11, Beutel and Vilhelmsen, 2007). A post-genal bridge (pgb, Figs. 1C and 2C) is not a groundplan feature of Hymenoptera, but probably evolved early in the group (e.g. Vilhelmsen, 1996; Beutel and Vilhelmsen, 2007). Whether the galeal crown (gacr, Figs. 5 and 6A) is a groundplan apomorphy of hymenoptera is not clear at present; a distal patch or row of setae on the galea was observed in basal representatives of Hymenoptera (Beutel and Vilhelmsen, 2007), but also in parasitic groups (Popovici et al., 2014) and members of Aculeata (Cowley, 1959).

Very few cephalic features link Formicidae with related groups of Aculeata. The maxillary comb (mxc, Figs. 5A and 6A) is probably generally present in ants and a row of setae in a very similar position also occurs in Vespidae (Duncan, 1939), Crabronidae (Cowley, 1959), and Scoliidae (Osten, 1982). Features of the mandibular base like the lateroventral process (abductor swelling, abs, Figs. 2D, 4C') that is internally connected to the adductor apodeme and the triangular processes of the distal postgenae (pgt, Fig. 2D) that mesally frame the mandibles are probably also part of the groundplan of Formicidae. These features are also described in Scoliidae (Osten, 1982) and *Pison* (Cowley 1959), but are missing in *Vespa* (Duncan 1939). A triangular process of the clypeus (vcpl, Fig. 2D) has not been described previously, but according to Osten (1982) the postgenal process occurs together with a ventral process of the clypeus in Scoliidae and other hymenopterans, which is arguably homologous to the triangular process described here. This is a potential derived character linking Formicidae with other Aculeata.

Generally, the inventory of cephalic muscles of ants is simplified compared to more basal hymenopteran lineages (Beutel and Vilhelmsen, 2007). In contrast, the inventory of cephalic muscles of Formicidae is very similar to what is found in members of their sister group Apoidea, for instance in *Pison* (Cowley, 1959; Zimmermann and Vilhelmsen, 2016) (see Table 1). They differ mostly in details of the arrangement caused by limited shifts of origins and insertions.

Formicidae is characterized by an entire series of autapomorphic cephalic features, complex evolutionary changes affecting most external and internal elements of the head. A conspicuous apomorphy in very clear contrast to other groups of Hymenoptera (e.g. Beutel and Vilhelmsen, 2007; Zimmermann and Vilhelmsen, 2016) is the prognathous orientation of the head. Frontal lobes (frl, Figs. 1A and 2A) and frontal carinae (frc, Figs. 1A and 2A) may be apomorphic groundplan features of Formicidae, the latter occur even in stem group ants such as Sphecomyrminae (Barden and Grimaldi, 2014), although they are indistinct or reduced in some groups. A feature strikingly differing from other hymenopterans is a labrum which can be interlocked with the maxillolabial complex (Fig. 10F, Keller, 2011). This configuration, which results in the formation of a tightly closed preoral cavity, is likely a complex apomorphy of Formicidae. An articulation with the stipes is arguably a groundplan apomorphy of Formicidae and an interlocking mechanism involving the palp a derived condition that evolved within the family (Keller, 2011). Also connected with the tight closure of the preoral space are modifications of the maxillolabial complex. In *W. affinis* a transverse groove of the prementum (pmtg, Figs. 5A and 7G) supports the interlocking with the labrum. This feature is variable within the Formicidae (Keller, 2011). Further modifications are the deep premental ditches (pmd, Figs. 5A and 7G) which interact with the mesal margins of the stipites. In *W. affinis* this interlocking is especially tight through the longitudinal grooves of the stipites (stgl, Fig. 5), which are part of a stipital groove that occurs very variably in the ants (Keller, 2011). The antennae and their articulation are also distinctly modified. A concave antennal insertion area (peritorular groove, ptg, Fig. 3D), a complex torulus (to, Figs. 1B, 2B and 3D, F) forming a sheath around the basal articulatory part of the scapus (Keller, 2011), and the geniculate shape of the antenna are likely another complex of autapomorphies of (crown)group ants. An alternative interpretation of the concave peritorular area would be that the face between the frontal carinae is raised, resulting in laterally oriented toruli. However, this state is lost in some groups, such as Leptanillinae (B. Boudinot, pers. obs.). The mandibles are also modified, with a secondary (dorsal) mandibular articulation (dma, Figs. 2A, C and 4D) that is formed like a gliding apparatus instead of the typical

**Table 1**

Comparison of the musculature of ants with several hymenopteran outgroup taxa. Muscle numbers are according to Beutel and Vilhelmsen (2007) (based on v. Kéler, 1963)/ Wipfler et al. (2011) or the respective reference for the taxon. +: muscle present, ++: muscle especially strongly developed, -: muscle absent, ?: Muscle is not described in the respective reference, but in comparison with other references it seems possible that it is present in the respective taxon, lm: Prepharyngeal longitudinal muscles, Mpe: *M. pharyngoepipharyngealis*.

Family	Xyelidae	Vespidae	Crabronidae	Formicidae	
Species	<i>Xyela julii</i>	<i>Vespa pensylvanica</i>	<i>Pison chilense</i>	<i>Wasmannia affinis</i>	<i>Neoponera villosa</i>
Reference	Beutel and Vilhelmsen (2007)	Duncan (1939)	Zimmermann and Vilhelmsen (2016)	present study	Paul et al. (2002)
M1/0an1	++	end	0an1	+	(18)
M2/0an2	+	ial	0an2	+	(17)
M3/0an3	+	eal	0an3	+	(18)
M4/0an4	+	iad	0an4	+	(17)
M5/0an6	+	?	?	+	?
M6/0an7	+	?	?	+	?
M7/0lb5	+	–	–	–	–
M9/0lb2	+	–	0lb 2	+	(19)
M11/0md1	+	admd	0md1	+	mc
M12/0md3	+	abmd	0md3	+	m0
M13/0md6	-?	?	0md8/0md6	+	?
M15/0mx1	+	pcd	0mx1	+	(11)
M17/0mx3	+	exm	0mx3/0mx 5	+	(13)
M18/0mx4	+	flst	0mx4	+	(12)
M19/0mx2	+	–	–	–	–
M20/0mx6	+	flc	0mx6	+	(15)
M21/0mx7	+	fga	0mx7	+	(14)
M22/0mx8	+	pdmp	0mx8	+	(16)
M23/0mx10	+	admp	–	–	–
M24/0mx12	+	?	?	+	?
M25/0mx13	+	–	–	–	–
M26/0mx14	+	–	–	–	–
M27/0mx15	-?	–	–	–	–
M28/0la8	+	–	–	–	–
M29/0la5	+	plad	0la5	+	(6)
M30/0la6	+	–	–	–	–
M31/0la11	+	pfli	0la11	+	(8)
M32/0la12	+	afli	0la12	+	(9)
M33/0la13	+	–	–	–	–
M34/0la14	+	dlbp	0la14	+	Palpus muscle
M35/0la16	+	?	?	+	?
M36/0la17	+	?	?	?	?
M37/0hy12	+	dmslv, pmslv	0hy12A + B	+	(10)
M38/0hy7	+	–	–	+	(9)
M41/0hy1	+	lphm	0hy1	+	(a/b)
M42/0bu2	+	fgpl	0hy3	+	(7)
M43/0ci1	+	a: cdmth, b: dlbc	0ci1, 0bu1?	+	(a/b)
M44/0bu1	–	dlbc	0bu1	+	(1)
M45/0bu2	+	1 dlph	0bu2	+	(1)
M46/0bu3	+	?	0bu3	+	?
M47/0hy2	–	–	0hy2	–	–
M48/0bu5	–	3 dlph?	0bu5	+	(1)?
M50/0bu6	–	3 dlph	0bu6	+	(1)
M51/0ph1	+	2 dlph	0ph1	–	?
M52/0ph2	+	4 dlph	0ph2	+	(2)
M67/0hy9	(67a++)	atim, ptim	?	+	(4)
M68/0st1	++	?	?	+	?
M69/0st2	+	dim	?	+	?
lm/Mpe	lm	pdmth	Mpe	+	(3)

ball and socket joint (e.g. Beutel et al., 2014). The torqued and triangular distal part of the mandible is certainly the prevalent type among extant ant species. This feature is shared with other aculeates such as Vespidae and various bee groups. However, many stem group ants and members of basal branches (e.g. *Apomyrma*, *Prionopelta*) show a diversity of mandibular shapes distinctly deviating from this type. It is apparent that a reliable evolutionary interpretation will require additional comparative studies (Barden and Grimaldi, 2016, B. Boudinot pers. obs.). Another potential apomorphy of the mandible is the mandalus (ma, Fig. 4C). Mandibular grooves and mandibular glands appear in many aculeate hymenopterans, however, the groove is not always associated with the gland opening and the gland opening is often not

shaped like the formicide mandalus (e.g. Hermann et al., 1971), the homologies are thus not entirely clear. The deep hypopharyngeal groove (hyg, Fig. 7A) with different surface properties is possibly autapomorphic for ants. It has been described by Gotwald (1969) as a general feature of the ant hypopharynx although his drawings are not detailed enough to determine, whether the structure of the groove is always developed in the same way as in *W. affinis*. In other hymenopterans a slight depression of the distal hypopharynx is described for example in *Vespa* (Duncan, 1939) and *Pison* (Cowley, 1959). This might consist a preceding stage of the hypopharyngeal groove of ants but more information is required to ascertain this. The entire anterior cephalic feeding apparatus is obviously highly modified in ants.

Several putative cephalic innovations require further clarification. The tentorium of ants is apparently strongly modified, with mesally directed lamellae (ml, Fig. 10A–C) of the anterior arms (ata, Fig. 10A–C) and lacking the ventrolateral lamellae of other aculeates such as *Sapyga* and *Pison* (Zimmermann and Vilhelmsen, 2016). Tentorial apomorphies also include distinctly reduced or missing dorsal arms, and also a secondary bridge which is largely or completely fused to the postgenae (e.g. Khalife et al., 2018: *Melissotarsus*), even though this condition also occurs in other groups of Aculeata (Zimmermann and Vilhelmsen, 2016). Information on more ant species including extinct ones and members of basal branches would be necessary to clarify the evolution of the tentorium. A potential autapomorphy of the digestive tract is a very sharp bend of the prepharynx (pph, Fig. 10F). A bent cibarium was coded as present for all aculeates as well as some other apocritans by Zimmermann and Vilhelmsen (2016). However, their illustrations (e.g. Fig. 7H) suggest that the bend is not quite as abrupt as in the investigated ant species. It is conceivable that the degree of bending of the prepharynx depends on the position of the maxillolabial complex. This could not be evaluated in the present study as the maxillolabial complex was retracted in all specimens. As in the case of other characters, detailed information on more species is required for a reliable interpretation. Another apomorphic feature of ant workers is the vestigial condition of the optic neuropils, which is obviously related with a more or less strongly reduced condition of the compound eyes.

The fragmentary information on the cephalic musculature of ants makes it almost impossible to assess the phylogenetic relevance of muscular features. The absence of *M. verticopharyngalis* (M. 51) is a potential autapomorphy of Formicidae. However, drawings in Lubbock (1877) suggest that a postcerebral dorsal pharyngeal dilator may be present in an unidentified formicine ant. The presence of M.41a in *Wasmannia* (Figs. 10D, 11FeH and 12A) (and *Acromyrmex*) is also difficult to interpret. This subunit of *M. frontohypopharyngalis* originates on the antennal insertion area (aphr, Fig. 10C) and inserts on the processes of the sitophore plate (spl, Fig. 12B). A similar muscle has not been described before, but it is possible that this unusual bundle has been overlooked in other species examined. Also possible is that this muscle is homologous to M. 47 (Ohy2, *M. tentoriooralis*) which originates on the clypeo-frontal ridge and inserts on the process of the sitophore plate (oral arm) in *Pison chilense* (Zimmermann and Vilhelmsen, 2016). In both cases a distinct shift of the origin of this muscle has to be assumed. The configuration of the mandibular adductor with a combination of different fibre types (Gronenberg et al., 1997) is certainly important in a functional context. However, the very fragmentary documentation does not allow a phylogenetic interpretation at present.

The optical system, including light sense organs and related parts of the brain (e.g. optic lobes), is a character system affected by dimorphism between winged sexual forms and wingless workers. Ocelli are usually distinctly developed in winged queens and males. They are also present in workers of some groups (e.g. several Formicinae genera), but are missing in workers of the majority of ant species (Keller, 2011). The size of the compound eyes is still relatively well-developed in the winged morphs, especially males, but distinctly reduced in size in workers or completely absent.

#### 4.4. Functional aspects

Head structures of ants vary considerably in correlation with different life habits (Hölldobler and Wilson, 1990). Gibb et al. (2015) described modifications linked with the trophic position and feeding habits of ant species. The mandibles likely show the widest spectrum of variation (Gotwald, 1969). In contrast, the inventory of

cephalic musculature of ants is remarkably conservative as far as presently known. While the musculature of the digestive tract is not well studied so far, the musculature of the mouthparts and antennae is generally the same in the different ants and many other aculeates studied so far (e.g. Lubbock, 1877; Janet, 1905, Table 1).

Ants show a wide variety of dietary preferences. Leaf cutting ants process plant parts and use them for fungiculture, there are numerous predaceous species, harvester ants which forage seeds, and also species relying on plants saps or sugary exudates of hemipterans (Hölldobler and Wilson, 1990; Kaspari, 2000). The typical ant mandible is characterized by a torqued and triangular distal part. This shape is likely suitable for different functions such as nest building, foraging, and also defence (Hölldobler and Wilson, 1990; Gronenberg et al., 1997). While many species deviate from the typical pattern, such as trap jaw ants (e.g. Larabee and Suarez, 2014), snap jaw ants (Gronenberg et al., 1998b; Larabee et al., 2018) and predators, such as *Myrmecia* (Gotwald, 1969), some of the largest ant genera including *Pheidole*, *Camponotus*, *Tetramorium*, and *Crematogaster* show the typical triangular, torqued mandible shape that can also be observed in *W. affinis* (Gotwald, 1969). All these genera are considered as predominantly “generalists” (Lach et al., 2010; Rosumek et al., 2018). It seems reasonable to assume that the triangular and torqued mandible is part of the ant groundplan. It does not only occur in the majority of ants (Gotwald, 1969; Keller, 2011) but also in some other groups of Aculeata, such as Vespidae (Keller, 2011). Gotwald (1969) speculated that this mandibular shape might be especially suitable for foraging and perhaps brood care, appearing to be well-suited to grasp objects such as larvae or food items. However, empirical evidence for this mechanical suitability is currently lacking. The torque of the mandible also allows the use of the maxillolabial complex while the mandible is closed, which might also be an advantage over the planar mandibular type. It is an interesting point that while the triangular, torqued mandible has obviously been very successful in the evolution of the group, extinct and extant Formicidae also exhibit a huge variability in their mandibular shapes (see e.g. discussion in Lattke et al., 2018). The mandible was possibly an important driver in ant evolution, an aspect that would certainly be interesting to explore further in future studies.

Not only the mandible itself, also the mandibular musculature varies among species, apparently in correlation with different feeding habits. The adductor (M. 11) was intensively investigated in several studies focused on functional morphology (Gronenberg et al., 1997; Paul and Gronenberg, 1999; Paul, 2001; Paul et al., 2002). A feature unknown in other groups of insects is the differentiation of different fibre types. A part of the fibres is directly attached on the apodeme. They are either specialized on rapid movements (usually with short sarcomeres) or on slow, powerful contractions (usually with long sarcomeres). Additionally, fibres with slow contraction properties which are attached on thread-like cuticular processes of the apodeme occur (Gronenberg et al., 1997). An obvious advantage is the distinctly increased origin area relative to the available insertion area (Paul and Gronenberg, 1999). The distribution of different fibre types varies strongly, and also the structure of the adductor apodeme and the attachment angles, which depend on the shape of the head capsule (Paul, 2001). Numerous fast fibres and only few fibres attached on threads are present in some specialised predators with elongated mandibles like *Myrmecia* and *Harpegnathos*. In contrast, directly inserted slow fibres are dominant in power-amplified trap-jaw ants of the genus *Odontomachus*, which are characterized by an elongated head and very long apodemes. After fixing the mandibles with the arresting mechanism of the ventral articulation, these fibres build up enormous force. Fast fibres on a specialized region of the apodeme are used to release the locking

mechanism which lead to a strongly accelerated mandible movement (Gronenberg, 1995). The  $\mu$ CT data sets available for this study allow only discrimination between directly and indirectly attached fibres. However, the distribution of different types can be estimated with a histological section series of *Wasmannia*. Even without precise measurements of the sarcomere length, the sections reveal that they are shorter in directly attached fibres. The distribution in the examined species is similar to that observed in the relatively closely related genus *Atta* by Gronenberg et al. (1997). Two rather small fast bundles that attach laterally and mesally on the apodeme are enclosed by numerous indirect fibres. The muscle as a whole is distinctly smaller in *Wasmannia*, comprises fewer fibers, and has a distinctly smaller area of origin. The size of the muscle in leaf cutting ants is apparently correlated with the energy-intensive activity of processing leaves (Roces and Lighten, 1995). The very similar arrangement of the muscles in *Atta*, *Acromyrmex* (unpublished observation A. Richter) and *Wasmannia* suggests that the distribution of fibre types might be phylogenetically conserved. However, more data are required for a reliable evaluation of this character system. Once more data are available it would also be interesting to further correlate different fiber types with the different mandibular shapes. Possibly, as the triangular torqued mandible is prevalent through most ants, there is also a certain fiber type distribution that has been especially successful within the group.

In contrast to the mandibles, the general configuration of the maxillolabial complex within Formicidae is largely conserved. One varying feature is the arrangement and shape of different types of setae (Gotwald, 1969). The interactions between the maxillae, labium and labrum also vary as shown here and especially by Keller (2011). The close connection between the different elements enables a strong retraction of the complex, which tightly closes the preoral space and guarantees independent movements of the mandibles. It is conceivable that this has contributed to the broad spectrum of morphological and functional variation of the mandibles. The maxillolabial complex is mainly used for food uptake and grooming (e.g. Gotwald, 1969). Different additional functions can occur, as for instance the maintenance of the fungal gardens in leaf cutting ants (e.g. Weber, 1972). Rows of setae and microtrichia on the labium, galea and lacinia likely play an important role in different functional contexts. Like species of most other groups of Hymenoptera, adult ants exclusively consume liquid food (e.g. Glancey et al., 1981). Small solid food particles are filtered by hairy structures of the epi- and hypopharynx and stored in the infra-buccal pouch. *Solenopsis invicta* female workers can filter all particles  $>0.88 \mu\text{m}$  (Glancey et al., 1981) and the smallest female workers of *Acromyrmex octospinosus* particles of  $10 \mu\text{m}$  diameter (Quinlan and Cherrett, 1978). Female workers of *Camponotus pennsylvanicus* filter particles larger than  $150 \mu\text{m}$ . However, by transferring food between female workers via trophallaxis and renewed filtration, they finally reach a distinctly smaller particle size (Eisner and Happ, 1962). According to Febvay and Kermarrec (1981), *A. octospinosus* also uses the lacinial combs to filter food in front of the functional mouth opening. A small pellet is formed in the infrabuccal pouch. It was assumed that it is regurgitated by female workers (e.g. Quinlan and Cherrett, 1978). However, Hansen et al. (1999) showed that *Camponotus modoc* Wheeler, 1910 digests at least a part of this substrate with gland secretions and bacteria. If this extraintestinal form of food processing plays a role in many ant species, the tightly closed preoral space might be advantageous in the context of this function. The uptake of liquids by ants was investigated by Paul and Roces (2003) and can function in two different ways, either through “sucking” or “licking”. All species examined so far can use both techniques on principle, although the preference varies according to species and situation.

The licking movement of the glossa is a combination of muscular force and inherent elasticity of the structure. Like in other groups of Hymenoptera, the glossa is retracted by contraction of *M. praementoglossalis* and *M. praementoparaglossalis* and extended by its inherent elasticity (e.g. Osten, 1982; Paul et al., 2002). The strongly developed prepharyngeal sucking pump described in the present work is certainly crucial for the uptake of liquid food. The surface structure of the glossa is also likely important for the functioning of the maxillolabial complex. The surface structure of the glossa of *W. affinis* is distinctly different from other investigated ants such as for instance *Acromyrmex* (unpublished observation A. Richter) and *Neoponera* (previously *Pachycondyla*) (Paul and Roces, 2003). Interestingly, the structure found in *A. aspersus* is similar to what is found in other representatives of Aculeata, like for instance *Vespa* (Baranek et al., 2018), whereas it differs distinctly in *W. affinis*. Reliable functional interpretations are presently not possible as the surface structure of the glossa of Formicidae is scarcely documented.

Considering Formicidae as a whole, selective pressure linked with feeding habits and other aspects of the biology had a major impact on the mandibles and their musculature. The less variable maxillolabial complex is a “multipurpose tool” for tasks important for all ants, especially for the uptake of liquid food and grooming.

The functional interpretations presented here should be considered as preliminary, but they serve to highlight how much we have to learn about the basic functional anatomy of this dominant group of insects. Further comparative studies of a broad sample of species representing the major formicid clades and considered in context of their variation in their sociobiology, ecology, and behaviour are required to understand anatomical variation and its functional significance. Such an effort to fully document the variation in ant morphology using next-generation imaging tools, and the causes and consequences of that variation, will increase our understanding of this evolutionary success story.

#### Author contributions

AR conducted the morphological documentation, prepared the figure plates and wrote the manuscript. AR, RGB, FBR and RAK conceptualized the study in its present form. RGB was involved in writing earlier and the final version of the manuscript. FBR, RAK, EPE and FHG also contributed to the text and made numerous comments and recommendations, which improved the study substantially. FBR collected the specimens and provided the  $\mu$ CT Scan. FHG uploaded the scan data. All authors read and approved the final version of the manuscript.

#### Acknowledgements

Great thanks are due to Benjamin Wipfler for his support with generating the 3D-reconstructions. We also want to thank Margarita Yavorskaya for her useful comments and help on preparing the mouthparts of small insects such as *W. affinis*. Everlasting gratitude is also due for Hans Pohl for his help with the sample preparation, SEM, Photomicrography and construction of the figure plates. Félix Baumgarten Rosumek was supported by a scholarship of the Brazilian National Council of Technological and Scientific Development (CNPq) (Brazil, grant number: 290075/2014-9). The  $\mu$ CT data were generated and made available in the context of the research project NOVA (Contact: Michael Heethoff, TU Darmstadt; Funding: BMBF programme “Research on condensed matter 2016–2019”) for cooperative use of tomographic datasets which is gratefully acknowledged. For the help with generating the scans we are also grateful to Sebastian Schmelzle. Great thanks are also due to

Brendon Boudinot and one anonymous reviewer who helped to significantly improve the work with their comments.

## Appendix A. Supplementary data

Supplementary data to this article can be found online at <https://doi.org/10.1016/j.asd.2019.02.002>.

## References

- Abouheif, E., Wray, G.A., 2002. Evolution of the gene network underlying wing polyphenism in ants. *Science* 297, 249–252. *AntWeb*. Available from: <http://www.antweb.org>. (Accessed 25 January 2019).
- Baranek, B., Kuba, K., Bauder, J., Krenn, H., 2018. Mouthpart dimorphism in male and female wasps of *Vespa vulgaris* and *Vespa germanica* (Vespidae, Hymenoptera). *Deutsche Entomologische Zeitschrift* 65, 65–74.
- Barden, P., 2017. Fossil ants (Hymenoptera: Formicidae): ancient diversity and the rise of modern lineages. *Myrmecol. News* 24, 1–30.
- Barden, P., Grimaldi, D., 2014. A diverse ant fauna from the mid-cretaceous of Myanmar (Hymenoptera: Formicidae). *PLoS One* 9, e93627.
- Barden, P., Grimaldi, D.A., 2016. Adaptive radiation in socially advanced stem-group ants from the cretaceous. *Curr. Biol.* 26, 515–521.
- Barden, P., Boudinot, B., Lucky, A., 2017. Where Fossils Dare and Males Matter: Combined Morphological and Molecular Analysis Untangles the Evolutionary History of the Spider Ant Genus *Leptomyrme* Mayr (Hymenoptera: Dolichoderinae). *Invertebrate Systematics* 31.
- Baroni Urbani, C., Bolton, B., Ward, P.S., 1992. The internal phylogeny of ants (Hymenoptera: Formicidae). *Syst. Entomol.* 17, 301–329.
- Beutel, R.G., Vilhelmsen, L., 2007. Head anatomy of xyelidae (Hexapoda: Hymenoptera) and phylogenetic implications. *Org. Divers. Evol.* 7, 207–230.
- Beutel, R.G., Krogmann, L., Vilhelmsen, L., 2008. The larval head morphology of *Xyela* sp. (Xyelidae, Hymenoptera) and its phylogenetic implications. *J. Zool. Syst. Evol. Res.* 46, 118–132.
- Beutel, R.G., Friedrich, F., Yang, X.-K., Ge, S.-Q., 2014. Insect Morphology and Phylogeny: a Textbook for Students of Entomology. Walter de Gruyter, Berlin.
- Beutel, R.G., Yan, E., Richter, A., Büsse, S., Miller, K.B., Yavorskaya, M., Wipfler, B., 2017. The head of *Heterogyrus milloti* (Coleoptera: Gyrimidae) and its phylogenetic implications. *Arthr. Syst. Phyl.* 75, 261–280.
- Blaimer, B.B., Brady, S.G., Schultz, T.R., Lloyd, M.W., Fisher, B.L., Ward, P.S., 2015. Phylogenomic methods outperform traditional multi-locus approaches in resolving deep evolutionary history: a case study of formicine ants. *BMC Evol. Biol.* 15, 271.
- Bolton, B., 2003. *Synopsis and Classification of Formicidae*. American Entomological Institute, Gainesville.
- Bolton, B., 2018. An Online Catalog of the Ants of the World. Available from: <http://antcat.org>. (Accessed 2 August 2018).
- Boonen, S., Billen, J., 2016. Functional morphology of the maxillary and propharyngeal glands of *Monomorium pharaonis* (L.). *Arthropod Struct. Dev.* 45, 325–332.
- Borowiec, M.L., Rabeling, C., Brady, S.G., Fisher, B.L., Schultz, T.R., Ward, P.S., 2017. Compositional heterogeneity and outgroup choice influence the internal phylogeny of the ants. *bioRxiv* 173393.
- Boudinot, B.E., 2013. The male genitalia of ants: musculature, homology, and functional morphology (Hymenoptera, Aculeata, Formicidae). *J. Hymenopt. Res.* 30, 29–49.
- Boudinot, B.E., 2015. Contributions to the knowledge of Formicidae (Hymenoptera, Aculeata): a new diagnosis of the family, the first global male-based key to subfamilies, and a treatment of early branching lineages. *Eur. J. Taxon.* 0.
- Brady, S.G., Ward, P.S., 2005. Morphological phylogeny of army ants and other dorylomorphs (Hymenoptera: Formicidae). *Syst. Entomol.* 30, 593–618.
- Brady, S.G., Schultz, T.R., Fisher, B.L., Ward, P.S., 2006. Evaluating alternative hypotheses for the early evolution and diversification of ants. *Proc. Natl. Acad. Sci. Unit. States Am.* 103, 18172–18177.
- Brandão, C.R.F., Mayhé-Nunes, A.J., 2007. A phylogenetic hypothesis for the *Trachymyrme* species groups, and the transition from fungus-growing to leaf-cutting in the Attini. *Adv. Ant Systemat. Hymenoptera Formicidae Homage EO Wilson* 50, 72–88.
- Brandão, C.R.F., Diniz, J.L.M., Feitosa, R.M., 2010. The venom apparatus and other morphological characters of the ant *Martialis heureka* (Hymenoptera, Formicidae, Martialinae). *Papeis Avulsos de Zoologia (São Paulo)* 50, 413–423.
- Brown, W., 1954. Remarks on the internal phylogeny and subfamily classification of the family Formicidae. *Insectes Sociaux* 1, 21–31.
- Brown Jr., W.L., Wilson, E.O., 1959. The evolution of the dacetinae ants. *Q. Rev. Biol.* 34, 278–294.
- Cavill, G., Robertson, P., Brophy, J., Duke, R., McDonald, J., Plant, W., 1984. Chemical ecology of the meat ant, *Iridomyrmex purpureus* sens. strict. *Insect Biochem.* 14, 505–513.
- Clark, D.B., Guayasamin, C., Pazmino, O., Donoso, C., de Villacs, Y.P., 1982. The tramp ant *Wasmannia auropunctata*: autecology and effects on ant diversity and distribution on Santa Cruz Island, Galapagos. *Biotropica*, pp. 196–207.
- Cowley, D.R., 1959. Studies on the Biology and Anatomy of *Pison spinolae* Shuckard (Hymenoptera, Sphecidae). Unpublished M.Sc. thesis. Auckland University, New Zealand.
- Currie, C.R., Poulsen, M., Mendenhall, J., Boomsma, J.J., Billen, J., 2006. Coevolved crypts and exocrine glands support mutualistic bacteria in fungus-growing ants. *Science* 311, 81–83.
- Duncan, C.D., 1939. Contribution to the Biology of North American Vespine Wasps. Stanford U. Press, Stanford U., California.
- Eisner, T., Happ, G., 1962. The infrabuccal pocket of a formicine ant: a social filtration device. *Psyche* 69, 107–116.
- Febvay, G., Kermarrec, A., 1981. Morphologie et fonctionnement du filtre infrabuccal chez une attine *Acromyrme octospinosus* (Reich) (Hymenoptera : Formicidae): rôle de la poche infrabuccale. *Int. J. Insect Morphol. Embryol.* 10, 441–449.
- Forbes, J., 1938. Anatomy and histology of the worker of *Camponotus herculeanus pennsylvanicus* de geer (Formicidae, Hymenoptera). *Ann. Entomol. Soc. Am.* 31, 181–195.
- Gibb, H., Stoklosa, J., Warton, D.I., Brown, A.M., Andrew, N.R., Cunningham, S.A., 2015. Does morphology predict trophic position and habitat use of ant species and assemblages? *Oecologia* 177, 519–531.
- Glancey, B.M., Vander Meer, R., Glover, A., Lofgren, C., Vinson, S., 1981. Filtration of microparticles from liquids ingested by the red imported fire ant *Solenopsis invicta* Buren. *Insectes Sociaux* 28, 395–401.
- Gotwald, W.H., 1969. Comparative Morphological Studies of the Ants: with Particular Reference to the Mouthparts (Hymenoptera: Formicidae). Agricultural Experiment Station, Ithaca (New York).
- Gotwald Jr., W.H., 1970. Mouthpart morphology of the ant *Aneuretus simoni*. *Ann. Entomol. Soc. Am.* 63, 950–952.
- Gotwald Jr., W.H., 1973. Mouthpart morphology of the african ant *Oecophylla longinoda* Latreille (Hymenoptera: Formicidae). *J. N. Y. Entomol. Soc.* 72–78.
- Grasso, D., Romani, R., Castracani, C., Viscchio, R., Mori, A., Isidoro, N., Le Moli, F., 2004. Mandible associated ants in queens of the slave-making ant *Polyergus rufescens* (Hymenoptera, Formicidae). *Insectes Sociaux* 51, 74–80.
- Grimaldi, D., Engel, M.S., 2005. *Evolution of the Insects*. Cambridge University Press, Cambridge.
- Gronenberg, W., 1995. The fast mandible strike in the trap-jaw ant *Odontomachus* I. Temporal properties and morphological characteristics. *J. Comp. Physiol. A* 176, 391–398.
- Gronenberg, W., 1996. The trap-jaw mechanism in the dacetinae ants *Daceton armigerum* and *Strumigenys* sp. *J. Exp. Biol.* 199, 2021–2033.
- Gronenberg, W., Ehmer, B., 1996. The mandible mechanism of the ant genus *Anochetus* (Hymenoptera, Formicidae) and the possible evolution of trap-jaws. *Zoology* 99, 153–162.
- Gronenberg, W., Paul, J., Just, S., Hölldobler, B., 1997. Mandible muscle fibers in ants: fast or powerful? *Cell Tissue Res.* 289, 347–361.
- Gronenberg, W., Brandão, C.R.F., Dietz, B.H., Just, S., 1998a. Trap-jaws revisited: the mandible mechanism of the ant *Acanthognathus*. *Physiol. Entomol.* 23, 227–240.
- Gronenberg, W., Hölldobler, B., Alpert, G.D., 1998b. Jaws that snap: control of mandible movements in the ant *Myrmica*. *J. Insect Physiol.* 44, 241–253.
- Hansen, L.D., Spangenberg, W.J., Gaver, M.M., 1999. The infrabuccal chamber of *Camponotus modoc* (Hymenoptera: Formicidae): ingestion, digestion, and survey of bacteria. In: *Proceedings 3rd International Conference on Urban Pests. Graficke zavody Hronov, Czech Republic*, pp. 211–219.
- Hashimoto, Y., 1990. Unique features of sensilla on the antennae of Formicidae (Hymenoptera). *Appl. Entomol. Zool.* 25, 491–501.
- Hashimoto, Y., 1996. Skeletomuscular modifications associated with the formation of an additional petiole on the anterior abdominal segments in aculeate Hymenoptera. *Jpn. J. Entomol.* 64, 340–356.
- Hermann, H.R., Hunt, A.N., Buren, W.F., 1971. Mandibular gland and mandibular groove in *Polistes annularis* (L.) and *Vespa maculata* (L.) (Hymenoptera: Vespidae). *Int. J. Insect Morphol. Embryol.* 1, 43–49.
- Hita Garcia, F., Fischer, G., Liu, C., Audisio, T.L., Alpert, G.D., Fisher, B.L., Economo, E.P., 2017a. X-Ray microtomography for ant taxonomy: an exploration and case study with two new *Terataner* (Hymenoptera, Formicidae, Myrmicinae) species from Madagascar. *PLoS One* 12, e0172641.
- Hita Garcia, F., Fischer, G., Liu, C., Audisio, T.L., Economo, E.P., 2017b. Next-generation morphological character discovery and evaluation: an X-ray micro-CT enhanced revision of the ant genus *Zasphectus* Wheeler (Hymenoptera, Formicidae, Dorylinae) in the Afrotropics. *ZooKeys* 693, 33–93.
- Hölldobler, B., Wilson, E.O., 1990. *The Ants*. Harvard University Press, Cambridge.
- Hölldobler, B., Stanton, R.C., Markl, H., 1978. Recruitment and food-retrieving behavior in *Novomessor* (Formicidae, Hymenoptera). *Behav. Ecol. Sociobiol.* 4, 163–181.
- Janet, C., 1899. Sur les nerfs céphaliques, les “corpora allata et le” “tentorium” de la fourmi (“*Myrmica rubra*” L.), Par Charles Janet. Société zoologique de France.
- Janet, C., 1905. Anatomie de la tête du *Lasius niger*. Limoges Imprimerie-Librairie Ducourtieux et Gout 1–40.
- Janicki, J., Narula, N., Ziegler, M., Guénard, B., Economo, E.P., 2016. Visualizing and interacting with large-volume biodiversity data using client-server web-mapping applications: the design and implementation of antmaps.org. *Ecol. Inf.* 32, 185–193.
- Jourdan, H., 1997. Threats on Pacific islands: the spread of the tramp ant *Wasmannia auropunctata* (Hymenoptera: Formicidae). *Pac. Conserv. Biol.* 3, 61–64.
- Kaspari, M., 2000. *A Primer on Ant Ecology*. Standard Methods for Measuring and Monitoring Biodiversity, Biological Diversity Handbook Series. Smithsonian Institution Press, Washington DC.

- Keller, R.A., 2011. A phylogenetic analysis of ant morphology (Hymenoptera: Formicidae) with special reference to the poneromorph subfamilies. *Bull. Am. Mus. Nat. Hist.* 355, 1–90.
- Kéler, S.v., 1963. *Entomologisches Wörterbuch, mit besonderer Berücksichtigung der morphologischen Terminologie.* Akademie-Verlag, Berlin.
- Khalife, A., Keller, R.A., Billen, J., Hita Garcia, F., Economo, E.P., Peeters, C., 2018. Skeletomuscular adaptations of head and legs of *Melissotarsus* ants for tunnelling through living wood. *Front. Zool.* 15, 30.
- Lach, L., Parr, C., Abbott, K., 2010. *Ant Ecology.* Oxford University Press, Oxford.
- Larabee, F.J., Suarez, A.V., 2014. The evolution and functional morphology of trap-jaw ants (Hymenoptera: Formicidae). *Myrmecol. News* 20, 25–36.
- Larabee, F.J., Gronenberg, W., Suarez, A.V., 2017. Performance, morphology and control of power-amplified mandibles in the trap-jaw ant *Myrmoteras* (Hymenoptera: Formicidae). *J. Exp. Biol.* 220, 3062–3071.
- Larabee, F.J., Smith, A.A., Suarez, A.V., 2018. Snap-jaw morphology is specialized for high-speed power amplification in the Dracula ant, *Mystridium camillae*. *R. Soc. Open Sci.* 5, 181447.
- Lattke, J., Delsinne, T., Alpert, G., Guerrero, R., 2018. Ants of the genus *Protalaridris* (Hymenoptera: Formicidae), more than just deadly mandibles. *EJE* 115, 268–295.
- Lee, C.-C., Wang, J., Matsuura, K., Yang, C.-C.S., 2018. The complete mitochondrial genome of yellow crazy ant, *Anoplolepis gracilipes* (Hymenoptera: Formicidae). *Mitochondrial DNA Part B* 3, 622–623.
- Liu, S.-P., Richter, A., Stöfel, A., Beutel, R.G., 2019. The mesosomal anatomy of *Myrmecia nigrocincta* workers and evolutionary transformations in Formicidae (Hymenoptera). *Arthropod Systematics and Phylogeny* (in press).
- Longino, J.T., Fernández, F., 2007. Taxonomic review of the genus *Wasmannia*. *Mem. Am. Entomol. Inst.* 80, 271–289.
- Lubbock, J., 1877. On some points in the anatomy of ants. *J. Microsc.* 18, 120–142.
- Michener, C.D., Fraser, A., 1978. A comparative anatomical study of mandibular structure in bees (Hymenoptera: Apoidea). *Univ. Kansas Sci. Bull.* 51, 463–482.
- Moreau, C.S., Bell, C.D., Vila, R., Archibald, S.B., Pierce, N.E., 2006. Phylogeny of the ants: diversification in the age of angiosperms. *Science* 312, 101–104.
- Muscadere, M.L., Traniello, J.F., Gronenberg, W., 2011. Coming of age in an ant colony: cephalic muscle maturation accompanies behavioral development in *Pheidole dentata*. *Naturwissenschaften* 98, 783–793.
- Osten, T., 1982. Vergleichend-funktionsmorphologische Untersuchungen der Kopfkapsel und der Mundwerkzeuge ausgewählter "Scolioidea" (Hymenoptera, Aculeata): mit 2 Tabellen. *Staatl. Museum für Naturkunde Stuttgart*.
- Paul, J., 2001. Mandible movements in ants. *Comp. Biochem. Physiol. Mol. Integr. Physiol.* 131, 7–20.
- Paul, J., Gronenberg, W., 1999. Optimizing force and velocity: mandible muscle fibre attachments in ants. *J. Exp. Biol.* 202, 797–808.
- Paul, J., Roces, F., 2003. Fluid intake rates in ants correlate with their feeding habits. *J. Insect Physiol.* 49, 347–357.
- Paul, J., Roces, F., Hölldobler, B., 2002. How do ants stick out their tongues? *J. Morphol.* 254, 39–52.
- Peregrine, D., Mudd, A., Cherrett, J., 1973. Anatomy and preliminary chemical analysis of the post-pharyngeal glands of the leaf-cutting ant, *Acromyrmex octospinosus* (Reich.) (Hym., Formicidae). *Insectes Sociaux* 20, 355–363.
- Perrault, G.H., 2005. ("2004"). Étude morphoanatomique et biométrique du métasoma antérieur des ouvrières. Contribution à la systématique de la phylogénie des fourmis (Hymenoptera: Formicidae). *Ann. Soc. Entomol. Fr. (n.s.)* 40, 291–371.
- Pohl, H., 2010. A scanning electron microscopy specimen holder for viewing different angles of a single specimen. *Microsc. Res. Tech.* 73, 1073–1076.
- Popovici, O., Miko, I., Seltmann, K., Deans, A., 2014. The maxillo-labial complex of *sparsion* (Hymenoptera, Platygastridae). *J. Hymenoptera Res.* 37, 77–111.
- Quinlan, R., Cherrett, J., 1978. Studies on the role of the infrabuccal pocket of the leaf-cutting ant *Acromyrmex octospinosus* (Reich.) (Hym., Formicidae). *Insectes Sociaux* 25, 237–245.
- Richter, A., Keller, R.A., Rosumek, F.B., Economo, E.P., Garcia, F.H., Beutel, R.G., 2019. Data from: The cephalic anatomy of workers of the ant species *Wasmannia affinis* (Formicidae, Hymenoptera, Insecta) and its evolutionary implications. *Arthropod Struct. Develop.*
- Roces, F., Lighten, J.R., 1995. Larger bites of leaf-cutting ants. *Nature* 373, 392.
- Rosumek, F.B., 2017. Natural history of ants: what we (do not) know about trophic and temporal niches of neotropical species. *Sociobiology* 64.
- Rosumek, F.B., Blüthgen, N., Brückner, A., Menzel, F., Gebauer, G., Heethoff, M., 2018. Unveiling community patterns and trophic niches of tropical and temperate ants using an integrative framework of field data, stable isotopes and fatty acids. *PeerJ* 6, e5467.
- Russell, J.A., Moreau, C.S., Goldman-Huertas, B., Fujiwara, M., Lohman, D.J., Pierce, N.E., 2009. Bacterial gut symbionts are tightly linked with the evolution of herbivory in ants. *Proc. Natl. Acad. Sci. Unit. States Am.* 106, 21236–21241.
- Saini, M.S., Dhillon, S.S., Aggarwal, R., 1982. Skeletomuscular differences in the thorax of winged and non-winged forms of *Camponotus camelinus* (Smith) (Hym., Formicidae). *Deutsche Entomologische Zeitschrift* 29, 447–458.
- Schoeters, E., Billen, J., 1996. The post-pharyngeal gland in *Dinoponera* ants (Hymenoptera: Formicidae): unusual morphology and changes during the secretory process. *Int. J. Insect Morphol. Embryol.* 25, 443–447.
- Schultz, T.R., Meier, R., 1995. A phylogenetic analysis of the fungus-growing ants (Hymenoptera: Formicidae: Attini) based on morphological characters of the larvae. *Syst. Entomol.* 20, 337–370.
- Snodgrass, R.E., 1935. *Principles of Insect Morphology.* Cornell University Press.
- Stork, N.E., 2018. How many species of insects and other terrestrial arthropods are there on earth? *Ann. Rev. Entomol.* 63, 31–45.
- Vilhelmsen, L., 1996. The preoral cavity of lower Hymenoptera (Insecta): comparative morphology and phylogenetic significance. *Zool. Scripta* 25, 143–170.
- Ward, P.S., 2014. The phylogeny and evolution of ants. *Annu. Rev. Ecol. Evol. Systemat.* 45, 23–43.
- Ward, P.S., Bolton, B., Brown, W.L., Shattuck, S.O., 1996. *A Bibliography of Ant Systematics.* Univ of California Press, Berkeley.
- Ward, P.S., Brady, S.G., Fisher, B.L., Schultz, T.R., 2010. Phylogeny and biogeography of dolichoderine ants: effects of data partitioning and relict taxa on historical inference. *Syst. Biol.* 59, 342–362.
- Ward, P.S., Brady, S.G., Fisher, B.L., Schultz, T.R., 2015. The evolution of myrmicine ants: phylogeny and biogeography of a hyperdiverse ant clade (Hymenoptera: Formicidae). *Syst. Entomol.* 40, 61–81.
- Weber, N.A., 1972. *Gardening Ants, the Attines.* American Philosophical Society.
- Webster, M.R., Socha, J.J., Teresi, L., Nardinocchi, P., De Vita, R., 2015. Structure of tracheae and the functional implications for collapse in the American cockroach. *Bioinspiration Biomimetics* 10, 066011.
- Wetterer, J.K., Porter, S.D., 2003. The little fire ant, *Wasmannia auropunctata*: distribution, impact, and control. *Sociobiology* 42, 1–42.
- Whelden, R.M., 1957a. Notes on the anatomy of *Rhytidoponera convexa* Mayr ("violacea" Forel) (Hymenoptera, Formicidae). *Ann. Entomol. Soc. Am.* 50, 271–282.
- Whelden, R.M., 1957b. Notes on the anatomy of the Formicidae I. *Stigmatomma pallipes* (Haldeman). *J. N. Y. Entomol. Soc.* 65, 1–21.
- Whelden, R.M., 1963. Anatomy of adult queen and workers of army ants *Eciton burckhelli* Westw. and *E. hamatum* Fabr. (Hymenoptera: Formicidae). *J. N. Y. Entomol. Soc.* 14–30.
- Wipfler, B., Machida, R., Müller, B., Beutel, R.G., 2011. On the head morphology of Grylloblattodea (Insecta) and the systematic position of the order, with a new nomenclature for the head muscles of Dicondylia. *Syst. Entomol.* 36, 241–266.
- Wipfler, B., Pohl, H., Yavorskaya, M.I., Beutel, R.G., 2016. A review of methods for analysing insect structures—the role of morphology in the age of phylogenomics. *Curr. Opin. Insect Sci.* 18, 60–68.
- Zimmermann, D., Vilhelmsen, L., 2016. The sister group of Aculeata (Hymenoptera) - evidence from internal head anatomy, with emphasis on the tentorium. *Arthropod Syst. Phylog.* 74, 195–218.